



HAL
open science

Asynchronous dynamics of the last Scandinavian Ice Sheet along the Pomeranian ice-marginal belt: A new scenario inferred from surface exposure ^{10}Be dating

Karol Tylmann, Vincent Rinterknecht, Piotr Woźniak, Valery Guillou

► To cite this version:

Karol Tylmann, Vincent Rinterknecht, Piotr Woźniak, Valery Guillou. Asynchronous dynamics of the last Scandinavian Ice Sheet along the Pomeranian ice-marginal belt: A new scenario inferred from surface exposure ^{10}Be dating. *Quaternary Science Reviews*, 2022, 294, pp.107755. 10.1016/j.quascirev.2022.107755 . hal-03871313

HAL Id: hal-03871313

<https://hal.science/hal-03871313v1>

Submitted on 25 Nov 2022

HAL is a multi-disciplinary open access archive for the deposit and dissemination of scientific research documents, whether they are published or not. The documents may come from teaching and research institutions in France or abroad, or from public or private research centers.

L'archive ouverte pluridisciplinaire **HAL**, est destinée au dépôt et à la diffusion de documents scientifiques de niveau recherche, publiés ou non, émanant des établissements d'enseignement et de recherche français ou étrangers, des laboratoires publics ou privés.

Asynchronous dynamics of the last Scandinavian Ice Sheet along the Pomeranian ice-marginal belt: A new scenario inferred from surface exposure ^{10}Be dating

Karol Tylmann ^{a, *}, Vincent R. Rinterknecht ^b, Piotr P. Woźniak ^c, Vallery Guillou ^b,
ASTER Team ^{b, 1}

^a University of Gdańsk, Faculty of Oceanography and Geography, Division of Geophysics, Piłsudskiego 46, 81-378, Gdynia, Poland

^b Aix Marseille Univ., CNRS, IRD, INRAE, CEREGE, Aix-en-Provence, France

^c University of Gdańsk, Faculty of Oceanography and Geography, Division of Geomorphology and Quaternary Geology, Gdańsk, Poland

ARTICLE INFO

Article history:

Received 29 April 2022

Received in revised form

22 August 2022

Accepted 31 August 2022

Available online xxx

Handling Editor: C. O'Cofaigh

Keywords:

^{10}Be surface exposure dating

Deglaciation

Pomeranian Phase

Scandinavian Ice Sheet

ABSTRACT

We present a new set of 25 ^{10}Be surface exposure ages of boulders located on the Pomeranian moraines and of erratic boulders located directly upstream of the Pomeranian moraines in northern Poland. Together with recalculated ^{10}Be surface exposure ages along the Pomeranian ice-marginal belt from Denmark to the west to Lithuania and Belarus to the east, the full data set ($n = 86$) enabled us to constrain the timing of the ice front standstill and its subsequent retreat. The investigated area consists of geomorphological record along ~2000 km of the ice margin associated with the ice sheet limit correlated so far with the Late Weichselian Pomeranian Phase (Bælthav in Denmark, Baltija in Lithuania and Braslav in Belarus).

We constrained deposition of the Pomeranian ice-marginal formations to discrete intervals: (1) ~20–19 ka in the area of the Baltic Ice Stream, (2) ~19–18 ka in the area of the Odra Ice Stream, (3) ~20–19 ka in the interstream zone between the Odra and the Vistula Ice Streams, (4) ~19–18 ka in the area of the Vistula Ice Stream, (5) ~18–17 ka in the area of the Mazury Ice Stream, (6) ~17–16 ka in the area of the Riga Ice Stream, and (7) ~16–15 ka in the area of the Novgorod Ice Stream. Our best age estimates are based on: (1) a minimum age of the ice margin retreat inferred from new and recalculated ^{10}Be ages of boulders as well as interpretation of available radiocarbon ages from organic deposits and OSL ages from sediments overlying tills, and (2) a maximum age of the ice margin stillstand and retreat inferred from interpretation of available OSL ages from sandur sediments deposited in front of the ice sheet. The asynchrony of the ice margin positions along the Pomeranian ice-marginal belt shows about 3–5 ka difference between the Bælthav ice margin in Denmark and the Braslav ice margin in Belarus. We propose a new scenario of the ice sheet evolution and a time-slice reconstruction of the last Scandinavian Ice Sheet's southern fringe for the period ~20–15 ka. We suggest that the term "Pomeranian Phase" should not be used but rather that the terms "Pomeranian moraines" or "Pomeranian ice-marginal belt" are adequate to describe geomorphological record of the palaeo-ice margin positions, which occurred during various phases of the last deglaciation.

© 2022 The Authors. Published by Elsevier Ltd. This is an open access article under the CC BY-NC-ND license (<http://creativecommons.org/licenses/by-nc-nd/4.0/>).

1. Introduction

In the area south of the Baltic Sea, the last Scandinavian Ice Sheet (SIS) formed distinct ice-marginal belts, traditionally ascribed

to the three MIS2 (in Europe the Late Weichselian) glacial phases: Brandenburg, Frankfurt and Pomeranian (Woldstedt, 1925, 1935). The ice-marginal landforms of the Brandenburg and the Frankfurt Phases are correlated with the maximum expansion of the last SIS in this region (e.g., Marks, 2012; Tylmann et al., 2019). During the ice sheet recession after the Local Last Glacial Maximum, a significant ice margin standstill occurred, which was so far correlated with the Pomeranian Phase. In northern Poland it is

* Corresponding author.

E-mail address: k.tylmann@ug.edu.pl (K. Tylmann).

¹ Georges Aumaître, Didier Bourlès and Karim Keddadouche.

morphologically expressed by well-defined terminal moraines, ice-contact sedimentary scarps or proximal edges of proglacial outwash fans/plains (e.g., Galon and Roszkówna, 1961; Roszkówna, 1968; Roman, 1990; Błazkiewicz, 1998; Kłysz, 2003) which may be correlated with similar landforms in: Denmark (e.g., Houmark-Nielsen, 2007, 2011), northern Germany (e.g., Bremer, 2000; Liedtke, 2001), Lithuania (Guobytė, 2004) and Belarus (Karabanov et al., 2004). This association of glacial marginal landforms has a complex origin: in some segments it was formed as a result of recessional standstill of the ice margin (e.g., Karczewski, 1989; Błazkiewicz, 1998, 2011), whereas in others the ice margin standstill occurred after re-advance of the ice front (e.g., Müller et al., 1995; Böse, 2005; Guobytė and Satkūnas, 2011). Nevertheless, based on the geomorphology, the Pomeranian ice-marginal belt may be traced across the southern sector of the last SIS as a relatively continuous record of the ice front position correlated with particular phases of deglaciation – Bælthav in Denmark, Pomeranian in Germany and Poland, Baltija in Lithuania, and Braslav in Belarus (cf. Liedtke, 1975; Houmark-Nielsen and Kjær, 2003; Karabanov and Matveyev, 2011; Guobytė and Satkūnas, 2011; Marks, 2015) (Fig. 1). In this regard, the Pomeranian ice margin is one of the most prominent ice-marginal features of the Weichselian glaciation in northern Europe (Lüthgens et al., 2011).

It is already well known that during the evolution of the last SIS, particular limits of the ice sheet were time-transgressive (cf. Hughes et al., 2021). The last SIS has never been still along its entire

ice margin at a given moment of time, as it is usually presented on traditional glaciomorphological maps, which usually display isochronous ice margin positions by connecting geomorphological features (e.g., Keilhack, 1901; Woldstedt, 1925; Liedtke, 1975). Due to dynamic behavior of particular ice streams and/or diversified response of the ice margin to changing climate, various sectors of the last SIS's southern front advanced and retreated differently over time resulting in a heterogeneous geomorphological record in the glacial landscape, which indeed reflects asynchronous events. To better understand the ice sheet dynamics, numerical dating of ice-marginal landforms could be a basis for new reconstructions of past asynchronous behavior (cf. Lüthgens and Böse, 2012).

Surface exposure dating with in-situ produced cosmogenic nuclides is routinely used in developing palaeo-ice sheet retreat chronologies (e.g., Corbett et al., 2017; Small et al., 2017; Rinterknecht et al., 2018; Barth et al., 2019; Tylmann et al., 2019; Dulfer et al., 2021). This technique offers direct numerical dating of glacial landforms, using mineral targets in stable erratic boulders resting at the ground surface. The advantage of this method for glacial geochronology is that moraines can be directly dated, instead of their age being constrained by radiocarbon dating of organic material and/or luminescence dating of sandy deposits intercalated between morainic sediments (Ivy-Ochs and Kober, 2008). In-situ cosmogenic nuclides were successfully used in constructing chronologies for MIS 2 palaeo-ice sheets (e.g., Marsella et al., 2000; Rinterknecht et al., 2006; Clark et al., 2009). In the

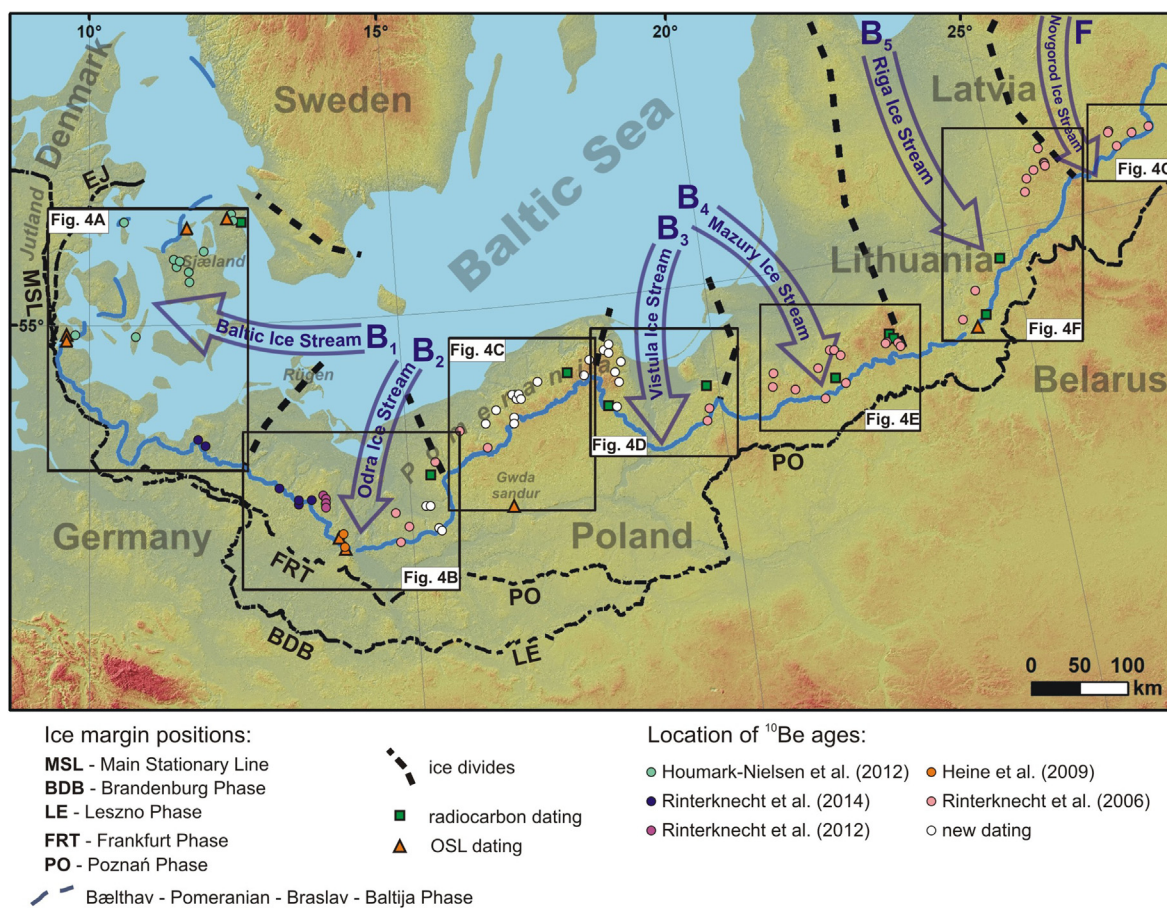


Fig. 1. The study area with reconstructed positions of the Late Weichselian (MIS 2) ice margins. The maximum expansion of the last SIS correlated with the Brandenburg (Leszno) and the Frankfurt (Poznan) Phases are indicated as well as a significant ice margin standstill, which was so far correlated with the Pomeranian Phase (light blue lines). Location of ¹⁰Be dating are marked with circles. Radiocarbon and OSL dating sites significant for the timing of the Pomeranian ice-marginal belt deposition are marked with squares and triangles, respectively. Digital elevation model based on SRTM data with a horizontal resolution of 80 m.

case of the vast southern periphery of the last SIS, a large chronological dataset is required to elucidate the full picture of former ice-marginal positions associated with multiple ice streams.

Here, we present a new set of 25 ^{10}Be surface exposure ages of boulders located on the Pomeranian moraines and of erratic boulders located directly upstream of the Pomeranian moraines in northern Poland. Together with recalculated ^{10}Be surface exposure ages along the Pomeranian ice-marginal belt, the full data set ($n = 86$) enabled us to constrain the timing of the ice front standstill and its subsequent retreat. In this study we provide the largest dataset of direct chronology for the southern periphery of the last SIS associated with the Pomeranian ice-marginal belt. This makes it possible to understand in details the behavior of an ice stream dominated ice margin in the context of climatic improvement and to understand the response of individual ice streams to local conditions. We propose a new history of ice-marginal oscillations and a time-slice reconstruction of the last SIS's southern fringe for the period $\sim 20\text{--}15$ ka. Our results provide a strong argument for the need to revise the pattern of the last deglaciation in the southern fringe of the SIS and define a new framework for the Late Weichselian glacial phases in the area south of the Baltic Sea.

2. Study area and dating targets

The study area covers the Pomeranian ice-marginal belt located south-west, south and south-east of the Baltic basin. It extends from Denmark in the west to Lithuania and Belarus in the east (Fig. 1). The ice sheet limit correlated so far with the Pomeranian Phase is easily traceable in the landscape of northern Europe. It is reconstructed based on the spatial arrangement of ice-marginal landforms, mainly: end moraines and distal outlets of tunnel valleys in Denmark (e.g., Houmark-Nielsen, 2007), end moraines and proximal edges of outwash plains in Germany and Poland (e.g., Liedtke, 2001; Marks, 2012) as well as end moraines and proglacial valleys in Lithuania (e.g., Guobytė and Satkūnas, 2011). The investigated area comprises geomorphological records spanning ~ 2000 km of the ice margin associated with the maximum ice sheet limit correlated so far with the Pomeranian Phase. The configuration of this palaeo-ice margin was shaped by the last SIS palaeo-ice streams operating within the southern periphery of the ice sheet (cf. Punkari, 1995; Boulton et al., 2001), what is revealed by the occurrence of distinct ice lobes, especially in the western segment of the ice margin (Fig. 1). Most of these palaeo-ice streams flowed westwards and southwards from the Baltic basin area. The western segment of the ice margin was shaped by the main Baltic Ice Stream (ice stream B_1 according to Punkari's classification) and the southern and eastern segment of the ice margin was shaped by the: Odra (B_2), Vistula (B_3), Mazury (B_4) and Riga (B_5) ice streams. The easternmost part of the ice margin was shaped by the Novgorod Ice Stream (F), which flowed from the east European Plain east of the Baltic basin (Fig. 1; Punkari, 1995).

^{10}Be dating targets were massive and intact boulders resting on glacial landforms correlated with the Pomeranian ice-marginal belt. We chose boulders located on landforms associated with the line indicating the maximum extent of the Pomeranian ice sheet and those located up to 50 km upstream of the ice sheet flow direction. The full set of ^{10}Be ages consists of 61 ages from boulders already dated in previous investigations (Rinterknecht et al., 2006, 2012, 2014; Heine et al., 2009; Houmark-Nielsen et al., 2012) and 25 new ages from boulders from northern Poland (Fig. 1). Sampled boulders are large and stable (embedded into the ground) granitic rocks significantly protruding (at least 0.9 m) above the ground surface (Fig. 2). We analyzed the distribution of all surface exposure ages ($n = 86$) and in a further step, we analyzed the distributions of ages obtained for boulders located within regions of individual ice



Fig. 2. Erratic boulder in northern Poland sampled for ^{10}Be dating (sample PM-30).

streams (Fig. 1). Moreover, we compared the results obtained for boulders located on the moraines indicating the maximum extent of the Pomeranian ice sheet, with results obtained for erratic boulders located up to 50 km upstream from the ice sheet maximum extent.

3. Methods

3.1. New samples

Samples were taken with a manual jackhammer from the upper surface of 25 boulders (PM samples) of height ranging from 0.9 to 3.8 m (Table 1). All boulders are characterized by quartz-rich lithologies as granitoids, granite gneisses and gneisses. In most cases one sample was taken per boulder. On a single occasion we collected two samples from a granitoid boulder with a quartz vein located in the area of the Odra Ice Stream. Sample PM-04A was taken from the granitoid rock, while sample PM-04B was taken from the quartz vein.

Sample preparation was conducted at the Laboratoire National des Nucléides Cosmogéniques in CEREGE, Aix-en-Provence, France. The rock samples were crushed and sieved. The 0.25–1.0 mm fraction was separated with a Frantz magnetic barrier laboratory separator in magnetic and non-magnetic subsamples. Several successive acid attacks of the non-magnetic fractions were performed using a mixture of concentrated hydrochloric acid (HCl) and fluorosilicic acid (H_2SiF_6). The purified quartz was decontaminated from meteoric ^{10}Be by three successive partial dissolutions with concentrated hydrofluoric acid (HF). Decontaminated quartz was dissolved with concentrated HF after adding 100 μL of an homemade ^9Be carrier solution ($[^9\text{Be}] = 3025 \pm 9$ g/g, μ Merchel et al., 2008). Beryllium was recovered after two successive separations on ion exchange columns: an anion exchange column (Dowex 1X8) to remove iron and a cation exchange column (Dowex 50WX8) to discard boron and recover Be (Merchel and Herpers, 1999). The eluted Be fractions were precipitated to $\text{Be}(\text{OH})_2$ with ammonia and oxidized to BeO. The BeO was mixed with niobium powder to prepare targets and the $^{10}\text{Be}/^9\text{Be}$ ratios were measured by accelerator mass spectrometry (AMS) at the French National AMS Facility ASTER, Aix-en-Provence (Arnold et al., 2010). The measured $^{10}\text{Be}/^9\text{Be}$ ratios were normalized relative to the in-house standard STD-11 using an assigned $^{10}\text{Be}/^9\text{Be}$ ratio of $(1.191 \pm 0.013) \times 10^{-11}$ (Braucher et al., 2015) and a ^{10}Be half-life of $(1.387 \pm 0.012) \times 10^{-6}$ years (Chmeleff et al., 2010; Korschinek et al., 2010). Analytical 1σ uncertainties include uncertainties in AMS counting statistics,

Table 1

Surface exposure ^{10}Be ages of erratic boulders located on the Pomeranian ice-marginal belt. The list consists of 25 new ^{10}Be ages (PM samples) and 61 ages recalculated from the original data of Heine et al. (2009), Houmark-Nielsen et al. (2012), Rinterknecht et al. (2006, 2012, 2014). All ^{10}Be exposure ages are calculated with 'Lm' time-dependent scaling scheme for spallation according to Lal (1991) and Stone (2000) and the global production rate according to Borchers et al. (2016).

Sample ID	Latitude N DD	Longitude E DD	Elevation (m a.s.l.)	Sample thickness (cm)	Shielding factor ^a	Quartz (g)	[^{10}Be] (10^4 at g^{-1})	Age (ka)
Baltic Ice Stream area								17.9 ± 0.7
SJAE-0705	55.4068	11.6268	45	2.0	1.0000	n.a.	6.29 ± 0.30	14.3 ± 1.3
SJAE-0706	55.9640	12.3500	20	2.5	1.0000	n.a.	8.89 ± 0.39	20.8 ± 1.8
SJAE-0707	55.4981	11.6044	35	3.0	1.0000	n.a.	6.96 ± 0.29	16.1 ± 1.4
SJAE-0708	55.5544	11.4090	50	3.0	1.0000	n.a.	7.25 ± 0.32	16.5 ± 1.4
SJAE-0709	55.6182	11.3859	35	3.5	1.0000	n.a.	9.04 ± 0.38	21.0 ± 1.8
SJAE-0710	55.6067	11.4725	45	4.0	1.0000	n.a.	8.18 ± 0.43	18.9 ± 1.7
SJAE-0711	55.6931	11.8703	15	4.0	1.0000	n.a.	5.92 ± 0.26	14.1 ± 1.2
SJAE-0712	56.0281	12.3609	40	2.0	1.0000	n.a.	8.85 ± 0.61	20.2 ± 2.1
FYN-0801	54.8972	10.7333	4	2.0	1.0000	n.a.	7.76 ± 0.36	18.5 ± 1.6
JYL-0803	54.9117	9.7618	50	2.0	1.0000	n.a.	1.59 ± 0.19	3.6 ± 0.5 ^b
JYL-0808	55.9785	10.5589	30	2.0	1.0000	n.a.	8.08 ± 0.31	18.6 ± 1.6
MVP-15	53.8658	11.8275	115	1.8	1.0000	31.4463	4.99 ± 0.87	10.6 ± 2.0 ^b
MVP-16	53.9272	11.7106	82	1.1	1.0000	32.4840	8.17 ± 0.36	17.9 ± 1.6
Odra Ice Stream area								16.6 ± 0.4
MVP-1	53.3272	13.4503	113	1.3	1.0000	34.2125	7.33 ± 0.51	15.6 ± 1.6
MVP-2	53.3244	13.2572	94	2.3	1.0000	5.6888	11.05 ± 2.52	24.2 ± 5.9 ^b
MVP-3	53.3042	13.2523	76	0.8	1.0000	13.1803	8.23 ± 0.54	18.2 ± 1.8
MVP-18	53.4494	12.9647	90	3.7	1.0000	30.5874	8.00 ± 0.82	17.8 ± 2.3
MVP-19	53.4503	12.9647	99	1.0	1.0000	31.1386	6.98 ± 0.42	15.0 ± 1.5
MVP-20	53.4503	12.9647	100	2.3	1.0000	25.3464	8.84 ± 0.41	19.2 ± 1.7
BER-97-01	53.3491	13.6505	82	2.0	0.9999	11.3085	7.53 ± 0.51	16.7 ± 1.7
BER-97-02	53.3250	13.6642	80	2.0	0.9884	25.6505	7.08 ± 0.36	15.9 ± 1.4
BER-97-03	53.2814	13.6364	91	2.0	0.9999	14.7713	6.01 ± 0.22	13.2 ± 1.1
BER-97-04	53.2629	13.6493	80	2.0	1.0000	17.2591	7.23 ± 0.43	16.0 ± 1.5
BER-97-05	53.2640	13.6480	60	2.0	1.0000	18.9498	7.49 ± 0.40	17.0 ± 1.6
PO-05-01	52.8800	13.9200	80	5.0	1.0000	n.a.	8.30 ± 0.39	17.3 ± 1.5
PO-05-02	52.9800	13.8700	73	3.0	1.0000	n.a.	9.20 ± 0.49	18.9 ± 1.7
PO-05-03	52.9800	13.8600	75	5.0	1.0000	n.a.	7.90 ± 0.29	16.5 ± 1.4
POM-12	52.8856	14.7914	80	1.0	1.0000	70.063	3.09 ± 0.30	7.1 ± 0.9 ^b
POM-13	52.8856	14.7914	80	1.0	1.0000	70.190	8.73 ± 0.62	20.1 ± 2.1
POM-16	53.1669	14.7358	96	1.5	1.0000	60.244	6.60 ± 0.47	15.0 ± 1.6
POM-17	53.0175	14.9544	60	1.5	1.0000	70.023	5.10 ± 0.40	12.0 ± 1.3
POM-18	53.6133	15.4369	102	1.0	1.0000	69.931	7.42 ± 0.78	16.6 ± 2.2
PM-01	53.2181	16.2552	62	3.0	0.9976	24.27	7.05 ± 0.36	16.1 ± 1.5
PM-02	53.2089	15.2299	60	1.6	1.0000	19.10	7.65 ± 0.57	17.3 ± 1.8
PM-03	53.2091	15.2299	60	1.2	1.0000	19.65	7.70 ± 0.61	17.3 ± 1.9
PM-04A	52.9963	15.4031	96	1.9	1.0000	24.75	8.63 ± 0.58	18.8 ± 1.9
PM-04B	52.9963	15.4031	96	2.0	1.0000	19.06	7.21 ± 0.56	15.8 ± 1.7
PM-04 ^c								17.2 ± 1.2
PM-05	52.9784	15.4213	95	2.5	1.0000	19.87	7.05 ± 0.47	15.5 ± 1.6
Odra/Vistula interstream area								17.6 ± 0.6
POM-21	53.7117	16.2553	133	2.0	1.0000	70.14	6.860 ± 0.510	15.0 ± 1.6
POM-22	53.8906	15.8381	110	1.5	1.0000	23.49	7.190 ± 0.650	16.0 ± 1.9
PM-08	53.9316	16.2611	75	3.2	1.0000	21.56	7.723 ± 0.656	17.3 ± 2.0
PM-09	53.9072	16.7199	174	2.8	0.9994	17.60	8.678 ± 0.687	17.6 ± 1.9
PM-10	53.9576	16.7262	181	1.2	0.9874	8.98	9.228 ± 0.690	18.5 ± 2.0
PM-11	54.0496	16.4278	100	3.5	0.9630	21.54	8.011 ± 0.552	18.2 ± 1.9
PM-12	54.1706	16.8343	119	1.4	1.0000	19.36	10.222 ± 0.572	21.6 ± 2.0
PM-13	54.1909	16.7664	110	1.2	0.9994	20.57	7.799 ± 0.454	16.6 ± 1.6
PM-14	54.1860	16.7453	113	3.8	1.0000	19.06	7.116 ± 0.403	15.4 ± 1.5
PM-15	54.1770	16.7886	115	2.3	1.0000	22.92	6.872 ± 0.521	14.7 ± 1.6
PM-16	54.2823	17.1412	137	1.7	1.0000	16.42	9.279 ± 1.044	19.3 ± 2.6
PM-17	54.2883	17.9010	248	2.6	0.9996	19.83	10.965 ± 0.512	20.5 ± 1.8
PM-20	54.4242	18.0064	192	2.0	1.0000	21.34	21.886 ± 2.205	43.2 ± 5.5 ^b
Vistula Ice Stream area								17.0 ± 0.8
POM-1	53.7236	19.7514	99	1.0	1.0000	72.519	9.210 ± 0.630	20.7 ± 2.1
POM-2	53.8444	19.8236	107	2.0	1.0000	70.065	6.810 ± 0.480	15.3 ± 1.6
PM-19	53.9621	18.3522	112	1.9	0.9872	13.84	8.979 ± 0.691	19.4 ± 2.1
PM-24	54.4910	18.2682	192	2.4	1.0000	24.57	15.598 ± 0.876	30.8 ± 2.9 ^b
PM-25	54.5126	18.2352	206	1.2	1.0000	19.96	8.068 ± 0.475	15.5 ± 1.5
PM-26	54.5465	18.3146	170	1.9	1.0000	25.60	9.019 ± 1.221	18.1 ± 2.8
PM-27	54.5038	18.2681	200	2.5	0.9939	27.62	7.659 ± 0.423	15.1 ± 1.4
PM-28	54.1910	18.4396	188	3.8	1.0000	20.92	6.388 ± 0.471	12.8 ± 1.4
PM-29	54.1910	18.4396	188	2.4	1.0000	18.34	9.006 ± 0.514	17.9 ± 1.7
PM-30	54.3006	18.4038	166	2.1	0.9997	20.96	12.482 ± 0.912	25.3 ± 2.7 ^b
PM-31	54.3932	18.5100	109	4.2	1.0000	22.11	8.336 ± 0.550	18.2 ± 1.8
Mazury Ice Stream area								16.4 ± 0.3
POM-3	54.0861	20.9097	117	2.0	1.0000	40.005	7.92 ± 0.58	17.6 ± 1.9
POM-4	53.9569	20.8597	167	1.5	1.0000	70.132	5.95 ± 0.42	12.5 ± 1.3 ^b
POM-5	53.9006	21.2028	175	2.0	1.0000	69.995	7.34 ± 0.61	15.4 ± 1.7

Table 1 (continued)

Sample ID	Latitude N DD	Longitude E DD	Elevation (m a.s.l.)	Sample thickness (cm)	Shielding factor ^a	Quartz (g)	[¹⁰ Be] (10 ⁴ at g ⁻¹)	Age (ka)
POM-8	54.0681	21.6097	138	3.0	1.0000	57.034	7.43 ± 0.65	16.3 ± 1.9
POM-10	54.1500	21.9958	173	1.0	1.0000	40.134	6.88 ± 0.55	14.3 ± 1.6
POM-11	53.9006	22.0167	177	1.0	1.0000	55.301	7.73 ± 0.53	16.0 ± 1.6
POL-1	53.7739	21.6286	117	2.0	1.0000	30.175	7.90 ± 0.71	17.6 ± 2.1
POL-1B	53.7739	21.6286	117	2.0	1.0000	30.021	7.17 ± 0.85	16.0 ± 2.2
POL-wm [^]								16.9 ± 1.7
POL-2	54.2147	21.8589	128	2.0	1.0000	30.861	7.71 ± 0.64	16.9 ± 1.9
POL-3	54.1950	21.9464	130	2.0	1.0000	29.988	11.97 ± 1.04	26.3 ± 3.0 ^b
POL-4	54.2358	22.7897	240	2.0	1.0000	30.267	8.39 ± 0.71	16.5 ± 1.9
POL-4B	54.2358	22.7897	240	2.0	1.0000	20.227	9.64 ± 1.14	18.9 ± 2.7
POL-4wm [^]								17.2 ± 1.7
POL-5	54.2039	22.7531	243	2.0	1.0000	30.180	8.32 ± 0.72	16.3 ± 1.9
POL-5B	54.2039	22.7531	243	2.0	1.0000	30.046	10.25 ± 1.22	20.1 ± 2.8
POL-5wm [^]								17.3 ± 1.7
POL-6	54.1647	22.9683	211	2.0	1.0000	28.208	41.06 ± 3.07	84.0 ± 9.1 ^b
POL-7	54.1642	22.9700	195	2.0	1.0000	30.066	10.10 ± 0.83	20.7 ± 2.3
POL-7B	54.1642	22.9700	195	2.0	1.0000	22.092	9.86 ± 1.00	20.2 ± 2.6
POL-7wm [^]								20.5 ± 1.9 ^b
Riga Ice Stream area								15.5 ± 0.5
BALTI-2	55.698	25.799	113	3.5	1.0000	52.864	6.72 ± 0.50	15.1 ± 1.6
BALTI-3	55.310	25.431	142	2.0	1.0000	69.716	7.41 ± 0.55	16.0 ± 1.7
BALTI-4	55.434	25.509	167	2.0	1.0000	60.775	7.84 ± 0.64	16.5 ± 1.8
BALTI-5	55.494	25.657	154	2.0	1.0000	49.123	6.19 ± 0.47	13.2 ± 1.4
LIT-2	55.544	25.846	187	2.0	1.0000	30.003	8.31 ± 0.73	17.1 ± 2.0
LIT-3	55.544	25.846	187	2.0	1.0000	29.995	7.55 ± 0.68	15.6 ± 1.8
LIT-3B	55.544	25.846	187	2.0	1.0000	30.434	9.70 ± 1.24	20.0 ± 3.0
LIT-3wm [^]								16.6 ± 1.7
LIT-8	54.273	24.021	190	3.8	1.0000	70.062	7.02 ± 0.56	14.7 ± 1.6
LIT-9	54.520	24.315	176	2.6	1.0000	48.370/	7.09 ± 0.54	14.9 ± 1.6
Novgorod Ice Stream area								14.7 ± 0.5
BEL-13	55.658	27.683	151	2.8	1.0000	71.447	7.18 ± 0.70	15.5 ± 1.9
BEL-14	55.639	27.375	150	1.7	1.0000	71.029	6.19 ± 0.47	13.2 ± 1.4
BEL-15	55.699	26.994	144	0.5	1.0000	29.117	6.99 ± 0.62	14.9 ± 1.7
BEL-15A	55.699	26.994	144	0.5	1.0000	34.198	7.39 ± 0.62	15.7 ± 1.8
BEL-16	55.544	27.076	152	2.0	1.0000	70.022	6.63 ± 0.46	14.2 ± 1.5

n.a. – not available.

Error-weighted mean age of two samples taken from one boulder.

^a Corresponding to self-shielding (direction and angle of surface dip).^b surface exposure ages not used (outliers) in calculation of the arithmetic mean with the standard deviation of the mean (italic).

uncertainty in the standard ¹⁰Be/⁹Be, an external AMS error of 0.5% (Arnold et al., 2010), and a chemical blank measurement.

¹⁰Be ages were calculated using the most recent global production rate (Borchers et al., 2016) and the time dependent scaling scheme for spallation according to Lal (1991) and Stone (2000) (the ‘Lm’ scaling scheme). We corrected the ¹⁰Be production rate for sample thickness according to an exponential function (Lal, 1991) and assuming an average density of 2.7 g/cm³ for granitoid, granite gneiss and gneiss. The appropriate correction for self-shielding (boulder geometry) was applied when the surface of the sampled boulder had a slope of more than 10°. No correction for the surface erosion of boulders was applied, as we interpret the ¹⁰Be results as minimum age for the ice sheet retreat. All calculations were performed using the online exposure age calculator formerly known as the CRONUS-Earth online exposure age calculator – version 3 (<http://hess.ess.washington.edu/math/>; accessed: January 21, 2022), which is an updated version of the online calculator described by (Balco et al., 2008). Ages are reported with 1σ uncertainties (including analytical uncertainties and the production rate uncertainty) in Table 1. Where two exposure ages are reported for one boulder (PM-04, PM-04B) the error-weighted mean age of two samples was calculated.

3.2. Recalculated ages

We recalculated ¹⁰Be ages already published for the Pomeranian ice-marginal belt (Rinterknecht et al., 2006, 2012, 2014; Heine et al.,

2009; Houmark-Nielsen et al., 2012) following the same procedure of exposure age calculations as described in section 3.1. Recalculated ¹⁰Be exposure ages are also reported with 1σ uncertainties (including analytical uncertainties and the production rate uncertainty) in Table 1. In the cases where two exposure ages are reported for one boulder (POL-1, POL-1B; POL-4, POL-4B; POL-5, POL-5B; POL-7; POL-7B; LIT-3, LIT-3B) the error-weighted mean age of two samples was calculated.

3.3. Timing for the ice margin positions

We estimated the most likely timing for the ice margin positions based on the following geochronological constraints:

- the arithmetic mean age and its uncertainty as the standard deviation of the mean for ¹⁰Be ages of boulders located within regions of particular ice streams (excluding outliers) interpreted as a minimum age of the ice margin retreat;
- the oldest radiocarbon ages from organic deposits and OSL ages from lacustrine, fluvial and fluvio-glacial deposits overlying Upper Weichselian tills associated with particular ice margin positions interpreted also as a minimum age of the ice margin retreat;
- the OSL ages from sandur sediments deposited in front of the Pomeranian ice-marginal belt interpreted as a maximum age of the ice margin stillstand and retreat.

Therefore, the most likely age of the ice margin positions is proposed as a time interval located between the minimum age of the ice margin retreat inferred from our ^{10}Be dataset and radiocarbon/OSL ages of deposits overlying till, and the maximum age of the ice margin stillstand and retreat inferred from OSL ages of sandur deposits. Details for the ice margin age estimation within regions of particular ice streams are described in section 5.1.

4. Results

4.1. Full ^{10}Be dataset ($n = 86$)

^{10}Be ages of boulders scattered along the Pomeranian ice-marginal belt range between 3.6 ± 0.5 ka and 84.0 ± 9.1 ka (Table 1), however the age range between 12.0 ± 1.3 ka and 21.6 ± 2.0 ka fall into a confidence interval arithmetic average $\pm 1.5 \times \text{IQR}$ (interquartile range, which is the range between the third quartile – Q3 and the first quartile – Q1 of the population) (Fig. 3). Variability of the ages falling into this confidence interval (12.7%) slightly exceeds the average analytical uncertainty (10.2%), suggesting that the random uncertainties are dominated by geological uncertainties rather than by analytical ones. The skewness is 0.17 indicating a slightly positively skewed distribution. The arithmetic mean of the 77 exposure ages is 16.7 ± 0.2 ka (standard deviation of the mean) (Fig. 3).

4.2. Baltic Ice Stream (B_1) area

Ages of boulders located in Denmark and northwest Germany, where the main Baltic Ice Stream (BIS) was located, range between 3.6 ± 0.5 ka and 21.0 ± 1.8 ka (Fig. 4A). Distribution of ages ($n = 13$) is polymodal with the main mode occurring around 18 ka. The reduced chi-squared test indicates that the ages are poorly clustered: $\chi_R^2 = 55.18$. We identify two of the youngest ages (3.6 ± 0.5 ka and 10.6 ± 2.0 ka) as deviating the most from the main mode. They do not fall into a confidence interval arithmetic average $\pm 1.5 \times \text{IQR}$, and are thus identified as outliers. These “too young” ages may be a result of boulders exhumation after deglaciation and/or significant postglacial erosion of the sampled surfaces. After excluding outliers, the remaining 11 ages range between 14.1 ± 1.2 ka and 21.0 ± 1.8 ka and a reduced chi-squared test shows a much better

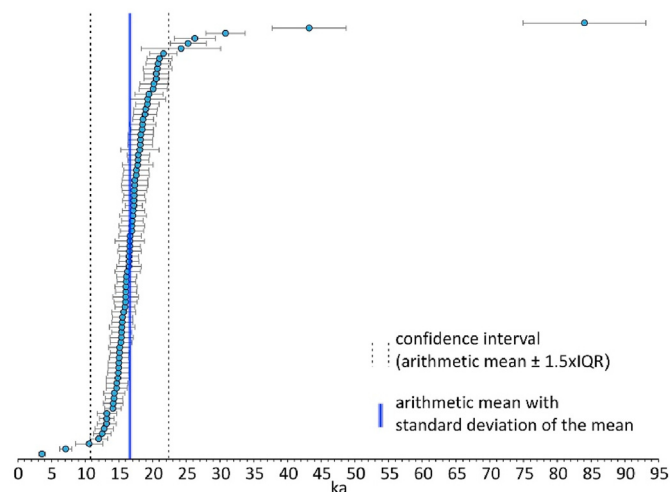


Fig. 3. Distribution of all ^{10}Be ages ($n = 86$) analyzed along the Pomeranian ice-marginal belt. The dataset consists of 25 new and 61 recalculated ages. The arithmetic mean age and the standard deviation of the mean are calculated for 77 exposure ages belonging to the confidence interval arithmetic mean $\pm 1.5 \times \text{IQR}$.

cluster: $\chi_R^2 = 2.76$. The variability of the remaining ages is 13.5%, with a $\chi_R^2 > 2$, and the dataset can be described as moderately clustered (Blomdin et al., 2016). The arithmetic mean and the standard deviation of the mean for these 11 surface exposure ages are 17.9 ± 0.7 ka (Fig. 4A).

Reliable ^{10}Be ages of boulders located on landforms associated with the line indicating the maximum extent of the Pomeranian ice sheet are 18.6 ± 1.6 ka and 17.9 ± 1.6 ka (with an arithmetic mean and a standard deviation of the mean of 18.2 ± 0.4 ka), while ^{10}Be ages of boulders located up to 50 km from this line upstream along former ice stream flowlines range between 14.1 ± 1.2 ka and 21.0 ± 1.8 ka (with an arithmetic mean and a standard deviation of the mean of 17.8 ± 0.9 ka). A t -test shows that for the 95% confidence level we cannot reject the hypothesis that these means are the same (p -value is 0.66). Thus, there is no significant difference between boulder ages on landforms associated with the line indicating the maximum extent of the ice sheet and those located up to 50 km within the ice stream pathway (Fig. 4A).

4.3. Odra Ice Stream (B_2) area

In the region where the Odra Ice Stream (OIS) was operating, the highest number of ^{10}Be ages were reported among all analyzed regions ($n = 24$). The ages range between 7.1 ± 0.9 ka and 24.2 ± 5.9 ka, and their distribution is relatively tight with the mode occurring around 16.5 ka (Fig. 4B). However, a reduced chi-squared test shows that these 24 ages are poorly clustered: $\chi_R^2 = 6.55$. The youngest age in the dataset (7.1 ± 0.9 ka) and the oldest (24.2 ± 5.9 ka) were identified as outliers – they lie beyond a confidence interval arithmetic average $\pm 1.5 \times \text{IQR}$. We invoke similar reasons as for the BIS to explain why one boulder is “too young”. For the boulder that is “too old”, it most probably contains beryllium inherited from episodes of exposure pre-dating the last deglaciation. After excluding these two outliers, the remaining 22 ages range between 12.0 ± 1.3 ka and 20.1 ± 2.1 ka with a reduced chi-squared test showing a cluster of 1.62. Because χ_R^2 is < 2 , and the variability of ages is $< 15\%$ (11.1%), we may describe this dataset as well clustered (Blomdin et al., 2016). The arithmetic mean and the standard deviation of the mean are 16.6 ± 0.4 ka (Fig. 4B).

Ten out of twenty-two ^{10}Be ages come from boulders located on landforms associated with the line delineating the maximum extent of the ice sheet. These ages range between 15.0 ± 1.5 ka and 20.1 ± 2.1 ka, with the arithmetic mean age and the standard deviation of the mean 17.3 ± 0.5 ka. ^{10}Be ages of erratic boulders located up to 50 km from this line upstream along former ice stream flowlines range between 12.0 ± 1.3 ka and 18.9 ± 1.7 ka, with the arithmetic mean age and the standard deviation of the mean 16.0 ± 0.5 ka (Fig. 4B). This slightly younger age of boulders located further to the north may reflect a progressive ice margin retreat. However, a t -test shows that for the 95% confidence level we cannot reject the hypothesis that the mean exposure age of boulders located on landforms associated with the maximum extent of the ice sheet and the mean exposure age of boulders located further to the north are the same (p -value is 0.09).

4.4. Odra/Vistula interstream area

In the interstream area between the OIS and the Vistula Ice Stream (VIS) ^{10}Be ages range between 14.7 ± 1.6 ka and 43.2 ± 5.5 ka ($n = 13$). The distribution is bimodal with the main mode occurring around 16–17 ka (Fig. 4C). The oldest age (43.2 ± 5.5 ka) clearly deviates from the rest of the data set, and it was identified as an outlier (age which lies beyond the confidence interval mentioned above). After removing this age from the dataset the

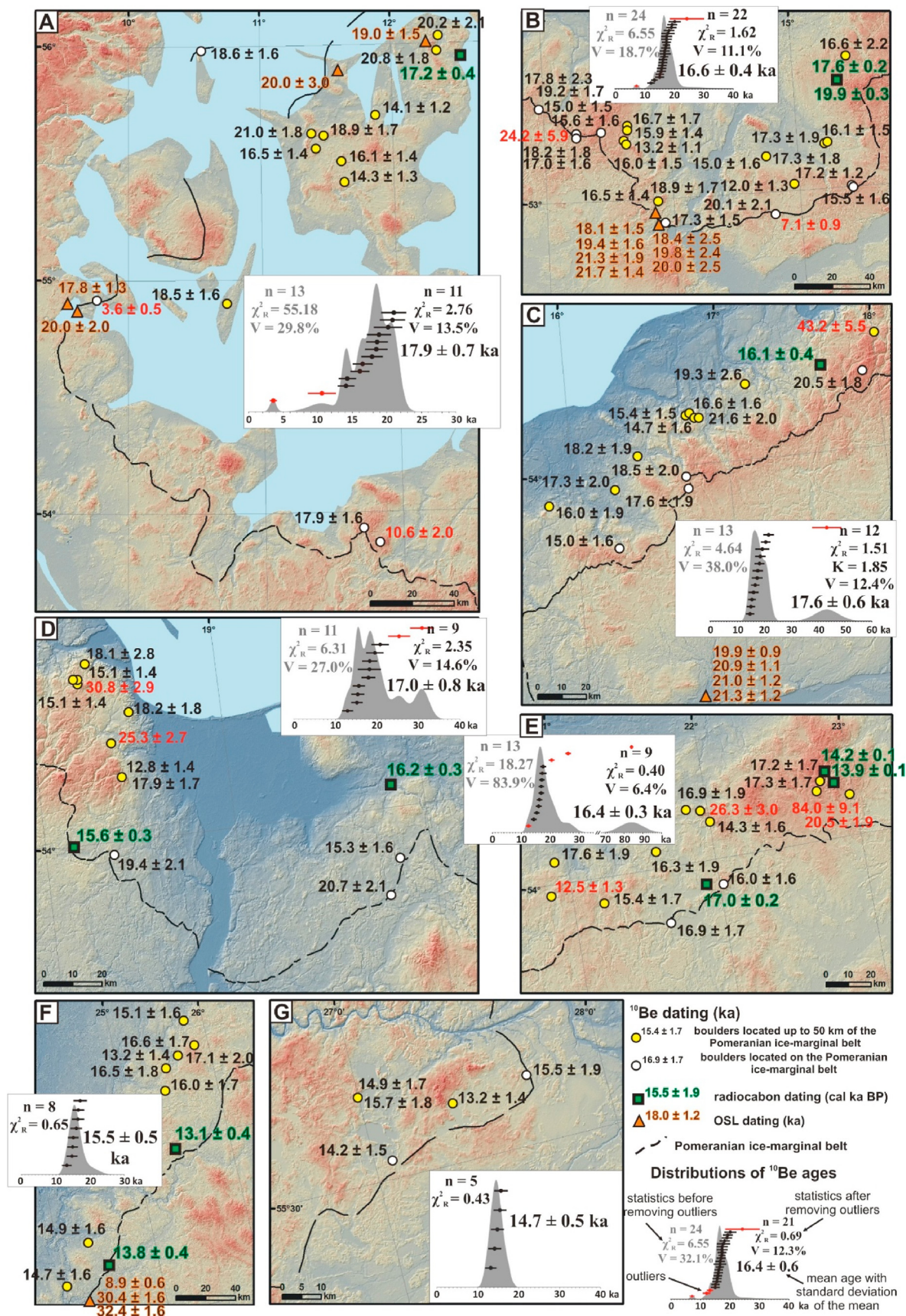


Fig. 4. Location of boulders dated with ¹⁰Be and distributions of ¹⁰Be ages within areas where particular ice streams were operating: (A) Baltic Ice Stream; (B) Odra Ice Stream; (C) Interstream area OIS/VIS; (D) Vistula Ice Stream; (E) Mazury Ice Stream; (F) Riga Ice Stream; (G) Novgorod Ice Stream.

distribution is unimodal and well clustered as indicated by the reduced chi-squared test: $\chi_R^2 = 1.51$. The ages range between 14.7 ± 1.6 ka and 21.6 ± 2.0 ka with a variability of 12.4%. The arithmetic mean and the standard deviation of the mean for 12 ages are 17.6 ± 0.6 ka (Fig. 4C).

^{10}Be ages of four boulders located on landforms associated with the line indicating the maximum extent of the Pomeranian ice sheet range between 15.0 ± 1.6 ka and 20.5 ± 1.8 ka (with an arithmetic mean age and a standard deviation of the mean of 17.9 ± 1.1 ka). ^{10}Be ages of eight boulders located up to 50 km from this line upstream the ice stream pathway range between 14.7 ± 1.6 ka and 21.6 ± 2.0 ka (with an arithmetic mean age and a standard deviation of the mean of 17.4 ± 0.8 ka). This shows that the mean ^{10}Be ages of boulders located on landforms associated with the line indicating the maximum extent of the ice sheet and those located up to 50 km from this line towards the interior of the ice sheet are coeval within the range of uncertainty (Fig. 4C). Moreover, a *t*-test shows that for the 95% confidence level we cannot reject the hypothesis that these means are the same (p-value is 0.73).

4.5. Vistula Ice Stream (B_3) area

In the region of the VIS we reported ages ranging between 12.8 ± 1.4 ka and 30.8 ± 2.9 ka ($n = 11$). The distribution is polymodal with a variability of 27% and a $\chi_R^2 = 6.67$ (Fig. 4D). We identify two outliers: 25.3 ± 2.7 ka and 30.8 ± 2.9 ka (ages which lie beyond the confidence interval arithmetic average $\pm 1.5 \times \text{IQR}$). When these ages are excluded, the remaining nine ages (from 12.8 ± 1.4 ka to 20.7 ± 2.1 ka) show a moderate cluster with variability of 14.6% and a $\chi_R^2 = 2.35$. The arithmetic mean and the standard deviation of the mean for these nine ages are 17.0 ± 0.8 ka (Fig. 4D).

^{10}Be ages of three boulders located on landforms associated with the maximum extent of the ice sheet are: 15.3 ± 1.6 ka, 19.4 ± 2.1 ka and 20.7 ± 2.1 ka (with an arithmetic mean age and a standard deviation of the mean of 18.5 ± 1.6 ka). ^{10}Be ages of six boulders located up to 50 km from this line upstream the ice stream pathway range between 12.8 ± 1.4 ka and 18.2 ± 1.8 ka (with an arithmetic mean age and a standard deviation of the mean of 16.3 ± 0.9 ka). The arithmetic means suggest a younger age for boulders located up to 50 km upstream the ice stream pathway (Fig. 4D). However, a *t*-test shows that for the 95% confidence level we cannot reject the hypothesis that these mean ages are the same (p-value is 0.32).

4.6. Mazury Ice Stream (B_4) area

Ages of boulders located in northeastern Poland, where the Mazury Ice Stream (MIS) influenced the ice margin position, range between 12.5 ± 1.3 ka and 84.0 ± 9.1 ka ($n = 13$). The distribution is bimodal, with the main mode occurring around 16–17 ka. The youngest age (12.5 ± 1.3 ka) and three of the oldest ages (84.0 ± 9.1 ka, 26.3 ± 3.0 ka and 20.5 ± 1.9 ka) do not fall into the confidence interval arithmetic average $\pm 1.5 \times \text{IQR}$. On this basis, these ages were identified as outliers (Fig. 4E). After removing these ages from the data set the distribution is unimodal and well clustered as indicated by a reduced chi-squared test χ_R^2 of 0.40 and variability of 6.4%. The ages range between 14.3 ± 1.6 ka and 17.6 ± 1.9 ka and the arithmetic mean and the standard deviation of the mean are 16.4 ± 0.3 ka (Fig. 4E).

Two out of nine ^{10}Be ages come from boulders located on landforms associated with the maximum extent of the ice sheet. The ages are 16.0 ± 1.6 ka and 16.9 ± 1.7 ka and the arithmetic mean age and the standard deviation of the mean are 16.5 ± 0.4 ka. ^{10}Be

ages of boulders located up to 50 km from this extent upstream the ice stream pathway range between 14.3 ± 1.6 ka and 17.6 ± 1.9 ka, with an arithmetic mean age and a standard deviation of the mean of 16.4 ± 0.4 ka. This shows that there is no significant difference between ages of boulders on landforms associated with the line indicating the maximum extent of the ice sheet and those located further upstream of the ice marginal position (Fig. 4E). It is also confirmed by a *t*-test, which shows that for the 95% confidence level we cannot reject the hypothesis that these mean ages are the same (p-value is 0.98).

4.7. Riga Ice Stream (B_5) area

In the region occupied by the Riga Ice Stream (RIS), we report ^{10}Be ages ranging between 13.2 ± 1.2 ka and 17.1 ± 2.0 ka ($n = 8$). There are no boulders located on landforms associated with the maximum extent, so all the ages come from boulders located up to 50 km north of the line indicating the maximum limit of the ice sheet upstream the ice stream pathway (Fig. 4F). The distribution is unimodal and well clustered as indicated by a reduced chi-squared test χ_R^2 of 0.65 and an age variability of 8.3%. No outliers were detected and the arithmetic mean age and the standard deviation of the mean are 15.5 ± 0.5 ka.

4.8. Novgorod Ice Stream (F) area

In the easternmost area of the Novgorod Ice Stream (NIS) ^{10}Be ages were reported ranging between 13.2 ± 1.4 ka and 15.7 ± 1.8 ka ($n = 5$). The distribution is unimodal and well clustered as indicated by a reduced chi-squared test χ_R^2 of 0.43 and an age variability of 6.9%. No outliers were detected and the arithmetic mean age and the standard deviation of the mean are 14.7 ± 0.5 ka (Fig. 4G).

Two out of five ^{10}Be ages come from boulders located on landforms associated with the maximum extent of the ice sheet. These ages are 14.2 ± 1.5 ka and 15.5 ± 1.9 ka with an arithmetic mean age and a standard deviation of the mean of 14.8 ± 0.6 ka. ^{10}Be ages of boulders located up to 50 km from this extent towards the interior of the ice sheet are 13.2 ± 1.4 ka, 14.9 ± 1.7 ka and 15.7 ± 1.8 ka, with an arithmetic mean age and a standard deviation of the mean of 14.6 ± 0.7 ka. These results show that there is no difference between the ages of boulders located on landforms associated with the line indicating the maximum extent of the ice sheet and those located further upstream to the north (Fig. 4G). It is also confirmed by a *t*-test, which demonstrates that at the 95% confidence level we cannot reject the hypothesis that these mean ages are the same (p-value is 0.82).

5. Discussion

5.1. Ages of the ice margin positions

Our results show that the most likely ages of ice margin positions correlated so far with the Pomeranian Phase of the Late Weichselian (Bælthav in Denmark, Baltija in Lithuania and Braslav in Belarus) vary between ~20 ka and ~15 ka along the southern front of the last SIS from the BIS region to the west to the sector of the NIS to the east (Fig. 5). We constrained the age of the ice margin position in the area occupied by the BIS to ~20–19 ka. This is based on the ^{10}Be minimum age of the ice margin retreat (17.9 ± 0.7 ka) as well as OSL ages of the Late Glacial lacustrine mud and fluvial sand overlying the Mid Danish and Young Baltic tills in Sjælland and southeast Jutland ranging between 20.0 ± 3.0 ka and 17.8 ± 1.3 ka (Fig. 4A; Houmark-Nielsen and Kjær, 2003). The oldest radiocarbon age of the Late Glacial lacustrine deposits overlying the Young Baltic

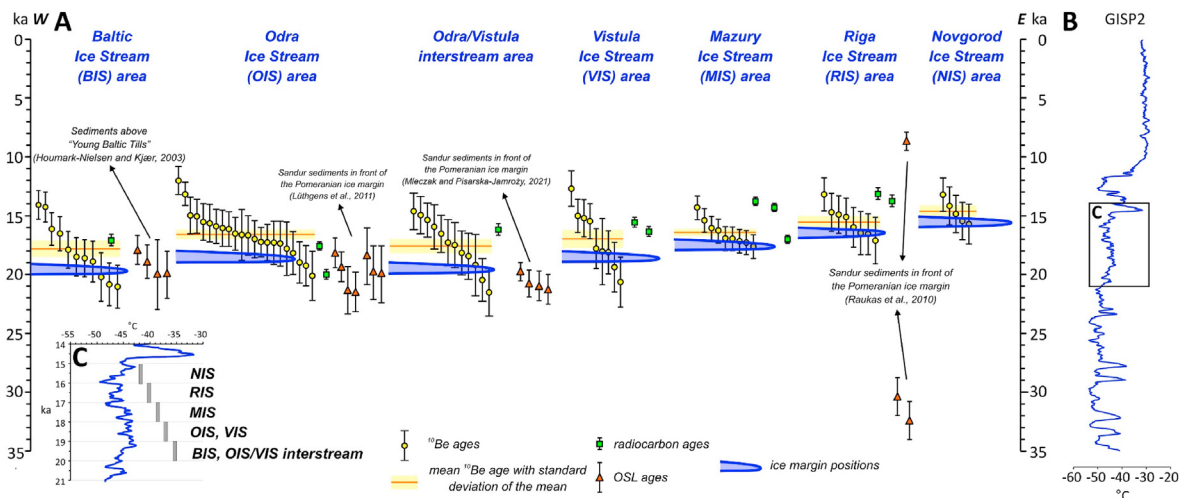


Fig. 5. (A) Timing of the ice margin positions along the Pomeranian ice-marginal belt. ^{10}Be ages used in mean surface exposure age calculations are shown against the radiocarbon and OSL ages significant for the timing of the Pomeranian ice margin positions. (B) Variability of palaeotemperatures inferred from the GISP2 ice core record (Alley, 2004) is shown for the period 0–35 ka. (C) Most probable ages of ice margin positions estimated in this study (grey bars) are shown against the palaeotemperature variability between 21 ka and 14 ka (Alley, 2004).

tills and within ice sheet extent of the Bælthav Phase is 17.2 ± 0.4 cal ka BP obtained from a bone found at the Nivå section in northeastern Sjælland (Table 2). If the age of the bone is equivalent to the age of deposits, it could suggest that the ice sheet retreat from the Bælthav ice marginal belt occurred earlier. Moreover, if the minimum age of ice margin retreat inferred from recalculated ^{10}Be dating is between 17.2 ka and 18.6 ka, the ice margin stillstand must have occurred earlier. Therefore, we interpret the age of the ice margin position in the area occupied by the BIS to ~20–19 ka as the most likely. However, if age of the Bælthav ice margin position is constrained to ~20–19 ka, then it is older than the timing of the ice re-advances after the recession from the Main Stationary Line (MSL) in Denmark. The latter (re-advances) were estimated based on lithostratigraphic and chronostratigraphic investigations of the Upper Weichselian sediments at 19–18 ka and 18–17 ka for the two Young Baltic advances which deposited the East Jylland and Bælthav ice-marginal formations (Houmark-Nielsen and Kjær, 2003; Krohn et al., 2009; Larsen et al., 2009). Stroeven et al. (2016) followed Houmark-Nielsen and Kjær (2003) when correlating the East Jylland with the Frankfurt and

Poznań ice-marginal formations, and the Bælthav with the Pomeranian ice-marginal formation in Germany and Poland, and constrained the isochronous retreat of the last SIS along the Bælthav ice-marginal belt to 18–17 ka. In the reconstruction of the last Eurasian ice sheet of Hughes et al. (2016) for the time-slice 19 ka the minimum ice extents are located within the area of the Bælthav ice-marginal belt. Furthermore, a thermomechanical ice sheet model for the retreat of the Eurasian ice sheet complex after 23 ka (Patton et al., 2017) shows that, in the optimal deglaciation scenario, the Bælthav ice-marginal formation lies mostly between of the 21 ka and 18 ka isochrones, which is supported by our age estimation in this sector of the ice sheet (Fig. 6A).

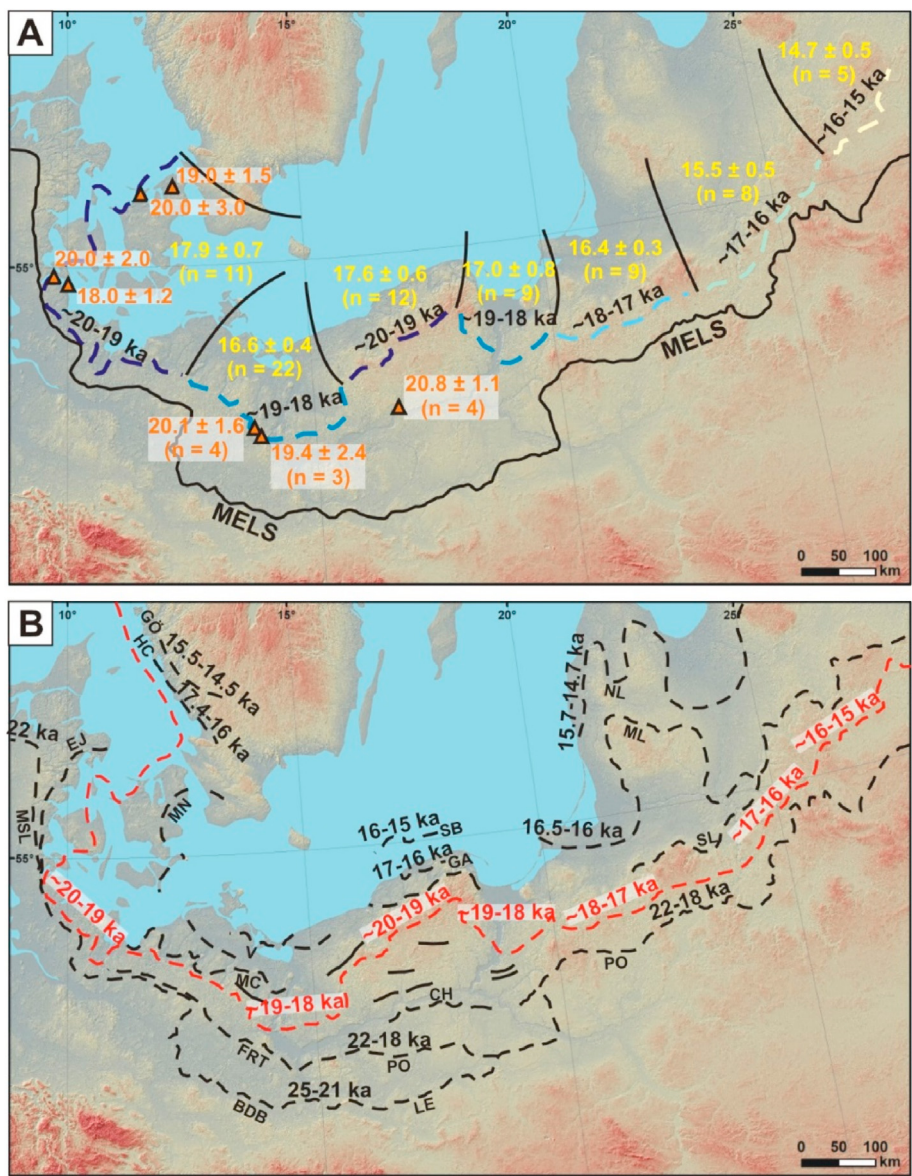
For the segment of the Pomeranian ice-marginal belt under the influence of the OIS (Figs. 1 and 4B), we constrained the most likely age of the ice margin position to ~19–18 ka (Fig. 5). The minimum age of the ice margin retreat calculated with all ^{10}Be ages in the region is 16.4 ± 0.4 ka. However, the mean ^{10}Be age of boulders located on landforms correlated with the maximum extent of the Pomeranian ice sheet is 17.3 ± 0.5 ka. Moreover, the oldest calibrated radiocarbon ages of organic deposits overlying a till, which

Table 2

Radiocarbon dates significant for constraining the minimum age of ice retreat from the Pomeranian ice-marginal belt. The conventional ^{14}C ages were calibrated with OxCal 4.4 according to IntCal20 calibration curve (Reimer et al., 2020).

Sample	Site	Dated material	Stratigraphic context	Method	^{14}C age [yr BP]	Calibrated age [cal ka BP]	References
Ua-1023	Nivå (section)	bone	Late Glacial lacustrine deposits	AMS	14 100 ± 300	17.16 ± 0.44	Lagerlund and Houmark-Nielsen (1993)
Gd-15891	Rega River (section)	carbonate	Late Glacial gyttja	conv.	14 430 ± 150	17.63 ± 0.23	Gliwice Radiocarbon Database (GRDB)
Gd-15907	Rega River (section)	carbonate	Late Glacial gyttja	conv.	16 450 ± 260	19.88 ± 0.32	Gliwice Radiocarbon Database (GRDB)
Gd-12636	Jasień Lake (core)	organic	Late Glacial gyttja	conv.	13 360 ± 240	16.10 ± 0.36	Gliwice Radiocarbon Database (GRDB)
Gd-6311	Boże Pole (section)	organic	Late glacial peat	conv.	13 010 ± 220	15.58 ± 0.34	Biaszkiewicz (1998)
Gd-10818	Stary Cieszyn (core)	organic	Late Glacial peat	conv.	13 420 ± 220	16.19 ± 0.33	Niewiarowski (2003)
GdA-137	Miłkowskie Lake (core)	plant macrofossil	Late Glacial lacustrine deposits	AMS	13 960 ± 100	16.95 ± 0.17	Czernik et al. (2009)
KIA33887	Hańcza Lake (core)	wood	Late Glacial lacustrine deposits	AMS	12 220 ± 45	14.15 ± 0.11	Lauterbach et al. (2011)
Poz-35959	Linówek Lake (core)	seeds	Late Glacial lacustrine deposits	AMS	11 690 ± 60	13.87 ± 0.10	Gałka and Sznal (2013)
n.a.	Bebrukas Lake (core)	organic	Late Glacial peat/gyttja	conv.	11 800 ± 300	13.80 ± 0.41	Neustadt (1971)
Mo-205	Vievis bog (core)	organic	Late Glacial peat	conv.	11 200 ± 340	13.14 ± 0.35	Serebryanny (1978)

n.a. – not available.



17.6 ± 0.6 (n = 12) mean surface exposure ^{10}Be age
 20.8 ± 1.1 (n = 4) mean OSL age
 $-18-17 \text{ ka}$ the Pomeranian ice-marginal belt with the most likely age of the ice margin position
MELS maximum extent of the last SIS

Ice-marginal belts:

- | | | |
|-----------------------------------|------------------------------|-------------------------------|
| MSL - Main Stationary Line | CH - Chodzież | ML - Middle Lithuanian |
| BDB - Brandenburg | MC - Mecklenburg | SL - South Lithuanian |
| LE - Leszno | V - Velgast | MN - Møn |
| EJ - East Jylland | GA - Gardno | HC - Halland coastal |
| FRT - Frankfurt | SB - Słupsk Bank | GÖ - Göteborg |
| PO - Poznań | NL - North Lithuanian | |

Fig. 6. Extents of the last SIS correlated previously with the Late Weichselian glacial phases and their ages. (A) Ages of ice margin positions along the Pomeranian ice-marginal belt. The best age estimates of ice margin positions within particular regions was constrained based on the mean ^{10}Be age of boulders and erratics, available OSL ages and the oldest radiocarbon ages (see Fig. 5). (B) Ages of the ice margin positions along the Pomeranian ice-marginal belt proposed in this study against the most likely ages for other Late Weichselian ice sheet limits known from the literature: Brandenburg (Leszno) and Frankfurt (Poznań) ice-marginal belts (Tylmann et al., 2019); Main Stationary Line (Houmark-Nielsen and Kjær, 2003; Larsen et al., 2009); Halland coastal and Göteborg moraines (Stroeven et al., 2016); Gardno and Stupsk Bank ice margins (Tylmann and Uścińowicz, 2022); Middle Lithuanian and South Lithuanian moraines (Kalm, 2006; Lasberg and Kalm, 2013).

may also indicate minimum age of deglaciation in this area, are 19.9 ± 0.3 and 17.6 ± 0.2 cal ka BP (Table 2; Fig. 4B). Based on OSL dating of sandur deposits, Lüthgens et al. (2011) constrained the age of the Pomeranian ice margin position in Germany between 20.1 ± 1.6 ka and 19.4 ± 2.4 ka (Fig. 5). This gives quite a wide time estimate based on various geochronological methods (from 20.1 to 16.4 ka). The reasons could be that: (1) ^{10}Be surface exposure dating may provide anomalous constraints for deglaciation due to "early" boulder exhumation in glacier termini during ice marginal retreat or "delayed" boulder exhumation during dead-ice melting and/or landform stabilisation following ice sheet retreat (cf. Houmark-Nielsen et al., 2012; Lüthgens et al., 2011); (2) radiocarbon dating of the oldest lacustrine/peat deposits of the lake basins located to the north of the ice-marginal belt also constrain the minimum age of deglaciation, as lake sediments started to accumulate as soon as dead ice melted (e.g., Błaszczewicz, 2011); however, in case of reworking of material for radiocarbon dating, ages could be "too old" and could be even older than the actual timing of the ice margin stillstand and retreat; (3) OSL dating of glacial deposits, such as sandur, constrains the timing of proglacial outwash deposition, which may have occurred before or during the ice-marginal stillstand but also possibly following ice-marginal retreat. Therefore, various dating techniques may constrain the timing of various processes occurring during ice margin stillstand and deglaciation, which may account for the wide range of obtained ages.

The maximum extent of the last SIS in eastern Germany and western Poland occurred during the Brandenburg (Leszno) Phase, not earlier than $\sim 25\text{--}24$ ka as indicated by calibrated radiocarbon ages of organic deposits underlying the Upper Weichselian till (e.g., Ehlers et al., 2011; Marks, 2012; Tylmann et al., 2019). OSL dating of sand underlying the upper most till at Rügen suggests, that the ice advance to the Late Weichselian maximum must have occurred between 25 ka and 21 ka (Kenzler et al., 2015, 2017; Pisarska-Jamroży et al., 2018). The retreat of the ice sheet from the maximum limit in eastern Germany occurred not later than 22.1 ± 0.9 ka as indicated by surface exposure ages from Brandenburg (Heine et al., 2009) recalculated with a global ^{10}Be production rate (Borchers et al., 2016). The Pomeranian ice margin position must thus post-date the phase of the maximum ice extent and also the phase of recessional ice margin stillstand (Frankfurt Phase). This is clearly inferred from morphostratigraphic relations between particular ice marginal belts (Fig. 6A and B). We propose an age of the Pomeranian ice-marginal position within the OIS region constrained to $\sim 19\text{--}18$ ka as the best age estimate. This corresponds to the minimum age of the Pomeranian ice sheet retreat from its maximum extent at 17.3 ± 0.5 ka. It overlaps with the age range of sandur deposits $21.7\text{--}17.0$ ka and partly agrees with the oldest radiocarbon ages of post glacial deposits. The radiocarbon ages (19.9 ± 0.3 and 17.6 ± 0.2 cal ka BP) may be however overestimated as bulk carbonate material (gyttja) was dated (Fig. 5; Table 2), opening the possibility that an age overestimation was caused by a freshwater reservoir effect related to water enriched in ancient dissolved calcium carbonates, the so called "hard water effect" (e.g., Philippsen, 2013).

In the central part of Pomerania in Poland, between the areas occupied by the OIS and the VIS (Figs. 1 and 4C) we constrained the most likely age of the Pomeranian ice margin position to $\sim 20\text{--}19$ ka. The minimum age for the ice margin retreat calculated based on ^{10}Be ages is 17.6 ± 0.6 ka, and it is comparable with the BIS mean ^{10}Be age obtained in the region (17.9 ± 0.7 ka). The oldest calibrated radiocarbon age of organic deposits formed after the ice margin retreated from the Pomeranian ice-marginal belt is 16.1 ± 0.4 cal ka BP (Table 2; Fig. 4C). However, the average age of outwash deposits from the distal part of the Gwda sandur deposited in front of the Pomeranian ice-marginal belt is 20.8 ± 1.1 ka (Mleczak and

Pisarska-Jamroży, 2021). This indicates that around $22\text{--}20$ ka the ice margin in this region was already situated to the north of the Frankfurt (Poznań) ice-marginal belt. The deposition of the Gwda sandur might have started during a progressive recession of the ice sheet after the Frankfurt (Poznań) Phase and before the ice margin stillstand along the Pomeranian ice-marginal belt. Taking into account the minimum age of deglaciation inferred from ^{10}Be ages and radiocarbon ages of lake deposits, as well as ages of the Gwda sandur deposits, we interpret the best age estimate for the ice margin position in central Pomerania to be $\sim 20\text{--}19$ ka.

We constrained the most likely age of the Pomeranian ice margin position to $\sim 19\text{--}18$ ka in the VIS region, based on the mean ^{10}Be age of all samples 17.0 ± 0.7 ka, the mean ^{10}Be age of boulders located on landforms associated with the line indicating maximum extent of the ice sheet 18.5 ± 1.6 ka ($n = 3$), and the oldest calibrated radiocarbon ages of organic deposits formed after the ice margin retreated 16.2 ± 0.3 and 15.6 ± 0.3 cal ka BP (Table 2; Fig. 4D). Taking into account the possible $22\text{--}18$ ka age of the local LGM in central and eastern Poland (Tylmann et al., 2019), it is likely that the age of the Pomeranian ice margin position in the VIS area is limited to $\sim 19\text{--}18$ ka (Fig. 6A and B). Similarly, our age constraints of $\sim 18\text{--}17$ ka in the MIS region, $\sim 17\text{--}16$ ka in the RIS region and $\sim 16\text{--}15$ ka in the NIS region are robust when we compare them with the most likely age of the last SIS maximum extent there (Fig. 6B). We inferred these constraints mainly from the mean ^{10}Be age of boulders and erratics supported by the oldest radiocarbon ages of sediments formed after the ice margin retreated (Fig. 4E–G). OSL ages of sandur deposits in front of the Pomeranian ice-marginal belt in the RIS region do not reflect the actual timing of the ice margin standstill (Raukas et al., 2010). Two ages (32.4 ± 1.6 and 30.4 ± 1.6 ka) are clearly too old (possibly due to incomplete bleaching of sediment grains) and one age (8.9 ± 0.6 ka) is much too young for the Upper Pleistocene deposits (Fig. 4F). One radiocarbon age from western Belarus (Zimenkov, 1989) provides an age for the last SIS maximum extent in the eastern part of the study area at ~ 22.5 cal ka BP (Tylmann et al., 2019). Surface exposure ^{10}Be ages of boulders and erratics located on and upstream the last SIS maximum extent in the Valday Heights (northwestern Russia, north east of the NIS region) constrained the timing (minimum age) of the local LGM to 20.1 ± 0.4 ka (Rinterknecht et al., 2018). The ages of the ice margin positions along the Pomeranian ice-marginal belt in the easternmost sectors of the study area are constrained to $\sim 17\text{--}16$ ka (RIS) and $\sim 16\text{--}15$ ka (NIS) which is significantly younger than the local LGM. We argue that these are the best age estimates based on available geochronological data. However, we are also aware, that the level of confidence with regard to the age of the ice margin positions in the RIS and NIS regions is lower than in the western sectors of the Pomeranian ice-marginal belt. This is because a larger number of various geochronological data (^{10}Be , OSL, ^{14}C) allowed us to constrain the possible timing of the ice margin stillstand in the western regions in comparison to the easternmost regions.

5.2. New scenario for ice margin positions and time-slice reconstruction ($\sim 20\text{--}15$ ka)

We propose a new scenario of the ice margin dynamics along the Pomeranian ice-marginal belt in the European Lowland (Fig. 7). The maximum extent of the last SIS in the area south of the Baltic basin occurred $\sim 25\text{--}22$ ka in the western sector of the ice sheet (Denmark, Germany, western Poland) during the Brandenburg (Leszno) Phase and $\sim 22\text{--}18$ ka in the eastern sector (central and eastern Poland, Lithuania, Belarus) during the Frankfurt (Poznań) Phase (Tylmann et al., 2019). After the local LGM the ice sheet started to retreat. However, during this period of general

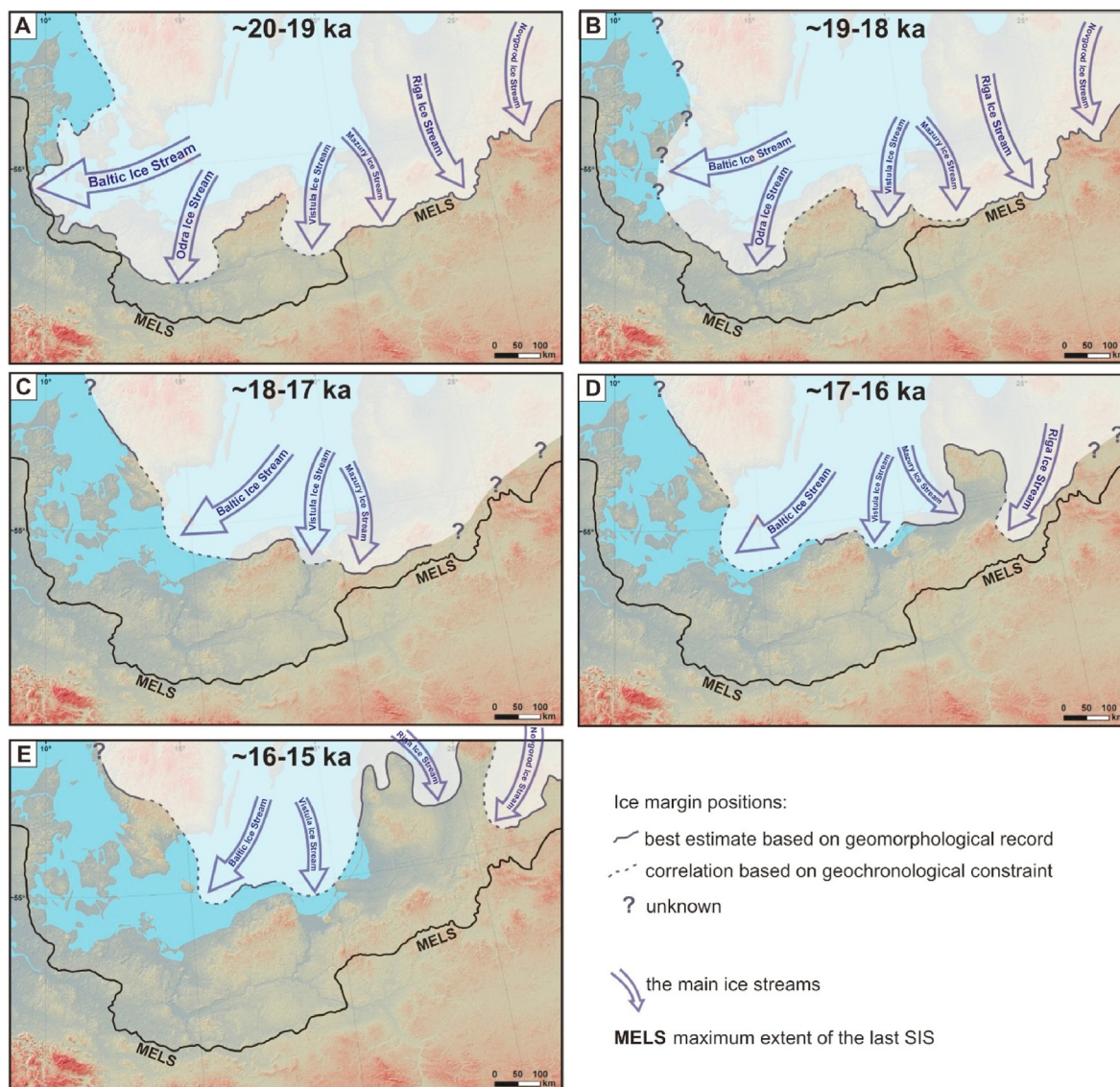


Fig. 7. Time-slice reconstruction of the southern SIS for the period ~20–15 ka. (A) Ice margin position around 20–19 ka. (B) Ice margin position around 19–18 ka. (C) Ice margin position around 18–17 ka. (D) Ice margin position around 17–16 ka. (E) Ice margin position around 16–15 ka.

deglaciation ice margin stillstands and/or local re-advances also occurred. The re-advances were most likely triggered by ice streams operating within the southern periphery of the last SIS. Most of these ice streams were located along the Baltic basin and were active not only during the ice sheet advance phase, but also during deglaciation (Punkari, 1995, 1997). The existence of several ice streams along the southern front of the last SIS was probably the main factor controlling the time-transgressive development of ice margins and diachronous formation of particular ice-marginal formations (e.g., Marks, 2002).

After recession of the ice margin from the Main Stationary Line in Denmark an ice re-advance occurred resulting in the formation of the Bælthav ice-marginal belt about 20–19 ka. Similar timing of the ice margin position was also estimated for the Pomeranian ice-marginal belt in central Pomerania in Poland. Age of the last SIS maximum extent in the eastern part of the study area may be roughly constrained to ~19–18 ka (e.g., Wysota et al., 2009; Marks, 2012; Larsen et al., 2016; Hughes et al., 2021), and in Germany, the age of the Frankfurt ice-marginal formation could be interpreted to

~20–18 ka (e.g., Litt et al., 2007; Marks, 2015). Thus, around 20–19 ka ago the ice margin was located along the Bælthav ice-marginal belt in Denmark and the Pomeranian ice-marginal formation in northwestern Germany. The ice sheet formed conspicuous ice lobes which terminated at the Frankfurt ice-marginal formation in northeastern Germany. In northwestern Poland, the eastern part of the ice lobe joined the Pomeranian ice-marginal belt of central Pomerania. Further to the east, the ice margin formed another ice lobe which probably linked the central Pomeranian ice margin with the maximum extent of the last SIS to the east (Fig. 7A). About 19–18 ka ago, the OIS and the VIS formed two conspicuous ice lobes in Poland (the Odra and Vistula Ice Lobes). The ice margin between the ice lobes was probably located in the northern part of Pomerania (interlobate zone). Location of the ice margin to the west of the OIS is difficult to reconstruct. East of the VIS, the ice margin most likely extended eastwards, merging with the local maximum extent of the last SIS (Fig. 7B).

About 18–17 ka ago, the ice margin was located at the Halland coastal moraine complex, which was recently dated to 17.4–16.0 ka

(Fig. 6B; Stroeven et al., 2016). The ice margin ran from the Halland coastal moraines to the southeast, across the Baltic basin, and was located along one of the recessional marginal belts in Pomerania in Poland. Further to the east, a small ice lobe could have linked this belt with the Pomeranian ice-marginal formation in the MIS region (Fig. 7C). The ice margin to the east of the MIS region at ~18–17 ka is more difficult to reconstruct, and its position remains rather unknown. Around 17–16 ka ago the ice margin was probably still located along the Halland coastal moraines. From there, it likely extended across the Baltic basin forming an extensive ice lobe, which terminated at the northern edge of Rügen and met the Gardno ice-marginal belt in the present coastal area of Poland (Fig. 7D). The existence of the ice lobe in the southwestern Baltic basin at that time was reconstructed based on possible extension of the Gardno ice-marginal belt at the seafloor along the present Polish coastline (cf. Uścińowicz, 1999), and on correlation of the Gardno moraines with the north Rügen moraines (Tylmann and Uścińowicz, 2022). To the east of the Gardno ice-marginal belt, the ice margin probably formed a small lobe, which linked this marginal formation with the western segment of the Middle Lithuanian moraines, dated to 16.5–16.0 ka (Fig. 6B) on the basis of calibrated radiocarbon ages and OSL ages (Kalm, 2006; Lasberg and Kalm, 2013). In the eastern sector of the study area a narrow ice lobe probably developed, linking the Middle Lithuanian moraines with the segment of the Pomeranian ice-marginal belt in the RIS region. The western flank of the ice lobe terminated at the Middle Lithuanian moraines, while the eastern flank terminated at the Pomeranian ice-marginal belt (Fig. 7D).

The last time-slice that we reconstructed is the most likely configuration of the ice margin at ~16–15 ka (Fig. 7E). In the western sector, the ice margin retreated from the Halland coastal moraines to the Göteborg moraines, which were recently dated to 15.5–14.5 ka (Fig. 6B; Lundqvist and Wohlfarth, 2001; Stroeven et al., 2016). To the southeast from the Göteborg moraines, the ice margin ran across the Baltic to the Stupsk Bank Phase ice-marginal belt reconstructed based on relicts of ice marginal landforms at the Baltic seafloor (e.g., Uścińowicz, 1999) and recently dated to ~15.2 ka (Uścińowicz et al., 2019) and 15.5 ± 0.5 ka (Tylmann and Uścińowicz, 2022). From the Stupsk Bank the ice margin most likely went northeast to the North Lithuanian ice-marginal belt, recently dated to 15.7–14.7 ka (Fig. 6B) based on calibrated radiocarbon ages and OSL ages (Kalm, 2006; Lasberg and Kalm, 2013). In the easternmost part of the study area the ice margin was linked by a narrow ice lobe to the segment of the Pomeranian ice-marginal belt formed by the NIS (Fig. 7E).

5.3. Asynchrony and asymmetry of the southern SIS

The asynchrony of the ice margin positions along the Pomeranian ice-marginal belt shows about 3–5 ka difference between the Bælthav ice margin in Denmark and the Braslav ice margin in Belarus (Fig. 6A). The general trend is that the ice margin positions become younger eastwards, except in central Pomerania in Poland, where the age of the ice margin position is similar to the age of the Bælthav ice margin in Denmark. To the west and to the east of central Pomerania in the OIS and VIS regions respectively, the Pomeranian ice-marginal belt is about 1 ka younger. The documented time-transgressive character of the Pomeranian ice-marginal belt was most likely caused by spatial and temporal variability of the last SIS dynamics triggered by activation and deactivation of particular ice streams (e.g., Stokes and Clark, 1999; Boulton et al., 2001). Comparison of the obtained chronology of ice margin positions to Greenland palaeotemperatures inferred from the GISP2 ice core record shows that the ice front stillstands along the Pomeranian ice-marginal belt occurred during relatively stable

climate period between cooling about 23 ka ago and significant warming about 14.5 ka ago (Fig. 5B). A closer look at the 21–14 ka interval in the GISP2 palaeotemperatures record reveals some minor coolings intervals occurring between 19 ka ago and 15 ka ago that may be correlated with the most likely age intervals of the ice margin positions in the OIS, VIS, MIS, RIS and NIS regions (Fig. 5C). However, activation and deactivation of ice streams along the southern periphery of the last SIS during this period was probably mostly controlled by regional and/or local factors rather than by the Northern Hemisphere climatic fluctuations.

Dynamics of various segments of the ice margin and particular ice streams could be related to regional and local climatic conditions occurring along the southern periphery of the last SIS or to local topographic and/or glaciologic parameters influencing the ice-marginal oscillations (e.g. facilitating ice streaming). Larsen et al. (2016) suggested that causes of the time-transgressive glacial maxima positions of the last SIS may be explained by glaciodynamic responses to geographically variable physical boundary conditions. Over a large area such as the southern periphery of the last SIS these variable conditions could be: (1) migration of the main ice divide during ice sheet build-up, (2) distance to ice-inception center, (3) topography and type of subglacial bed or (4) thermal regime at the ice/bed interface and ice flow mechanisms. Some of these factors are climatically driven (e.g. windward ice sheet growth), whereas others are purely local (e.g. topography and type of subglacial bed).

Variable timing of the ice margin stillstands along the Pomeranian ice-marginal belt is to some extent a continuation of the time-transgressive glacial maxima positions (Larsen et al., 2016; Hughes et al., 2021) as the Pomeranian ice-marginal landforms were formed during the general recession of the last SIS from its last maximum extent. Another factor could be related to varying distances to former ice dispersal centers, which for the eastern segment of the ice margin was greater than for the western sector. This could have possibly delayed ice sheet expansion in the eastern sector. In Russia, north east of the Valday Heights, the maximum extent of the last SIS in the area of the river Dvina ice lobe could occur as late as about 17–16 ka ago (Larsen et al., 2014). This is significantly later than the local Last Glacial Maximum in the area south of the Baltic Sea, which is estimated at 25–21 ka ago in the western segment of the ice margin and 22–18 ka ago in the eastern segment (Fig. 6B; Tylmann et al., 2019). This confirms the younger age of ice margin positions of the last deglaciation eastwards, what is typical both for the maximum extent and for recessional stages.

The western segment of the ice margin retreated largely within the Baltic basin, where extensive ice-dammed lakes were formed in front of the ice sheet in early stages of the last deglaciation. These lakes tended to merge and form one extensive ice-dammed lake, which periodically had connections with the ocean in the later stages as the ice margin was progressively retreating to the north (e.g., Uścińowicz, 1999; Andrén, 2012). This may account for the more dynamical behavior of the lake/marine terminating ice margin in comparison to the mainly land-based (and potentially cold-based) eastern sectors (Larsen et al., 2016). However, in the eastern sectors local ice-dammed lakes also occurred (e.g., Larsen et al., 2014; Gorchach et al., 2017) but the influence of these proglacial lakes was probably more local and confined to the river valleys and narrow, long, low-gradient lobes, such as the river Dvina ice lobe (Larsen et al., 2014).

The influence of ice bed topography was probably significant for the asynchronous behavior of the Pomeranian ice margin in the OIS and VIS regions, and in the interlobate area between them. OIS and VIS flowed along the large, N–S oriented valleys of the Odra and Vistula rivers. These valleys most likely already occurred in the last SIS's bed topography, as their origin predates the last glaciation

(Kordowski, 2009; Hermanowski, 2015). Large, elongated depression at the ice/bed interface could facilitate ice streaming and dynamic oscillations of the ice margins in these regions due to faster ice advances, formation of over-extended ice lobes and rapid ice margin recessions. On the other hand, the Pomeranian region between OIS and VIS is characterized by relatively highly elevated upland area, which could be an obstacle for slower advancing ice, but also a zone of slower ice margin recession, and as a consequence, a more stable ice margin position (Fig. 7A, B, C and D). Similarly, highly-elevated uplands of Lithuania and Latvia probably also controlled the distribution of the MIS, RIS and NIS in the eastern part of the study area (Fig. 7D and E).

The time-slice reconstruction shows that the southern periphery of the last SIS during the period 20–15 ka is characterized by a clear asymmetry: the western sector retreated earlier and much further to the north from the line of the maximum extent than the eastern sector (Fig. 7). Moreover, in the western sector of the southern SIS many more ice margin positions are recorded in the landscape compare to the eastern sector (Fig. 6B). During the time-slice 20–19 ka in the western sector of the study area, the ice margin was located almost at the same place as the maximum extent of the last SIS or up to ~30 km away from it, while in the eastern sector the ice sheet was at its maximum extent (Fig. 7A). During the time-slice 16–15 ka in the western sector of the study area, the ice margin was already located as far as ~230–360 km from the maximum extent of the last SIS, while in the eastern periphery of the study area the ice margin was only ~60–85 km from the maximum extent (Fig. 7E). This highlights that for the period ~20–15 ka the western sector of the ice margin was much more dynamic than the eastern sector. The difference could be a response of the ice sheet to the maritime climate influences from the west and/or a response to the local conditions such as presence of extensive proglacial lakes in front of the ice margin as well as the possible dominance of warm ice in the western sector of the southern SIS.

5.4. Implications for deglaciation pattern and outlook

Our new glacial chronology along the Pomeranian ice marginal-belt and the proposed time-slice reconstruction for the southern periphery of the last SIS questioned the existing framework of the last deglaciation phases in this region. The traditional glacial phases of the Late Weichselian in the area of Middle Europe (Brandenburg, Frankfurt and Pomeranian) were introduced by Prussian geologists, who at the beginning of the 20th century developed glaciomorphological maps with stages/phases of deglaciation inferred from spatial distribution of ice-marginal landforms such as end moraines and ice-marginal valleys – Urstromtäler (Keilhack, 1901, 1909; Wahnschaffe, 1905; Woldstedt, 1925). This relative chronology of deglaciation stages/phases was simply based on morphostratigraphic evidences at first. In the later years, this pioneering picture of the last SIS retreat was supplemented with detailed spatial distribution of ice-marginal formations and/or introducing additional stages/phases of deglaciation in particular regions (e.g., Roszko, 1955; Galon and Roszkówna, 1961; Pachucki, 1961; Mojski, 1968; Liedtke, 1975; Kozarski, 1981; Wysota, 1999). The next key step was taken when radiocarbon dating of organic deposits associated with glacial sediments and landforms enabled for the first time to give a chronological frame to particular deglaciation stages/phases (e.g., Cepek, 1965; Kozarski, 1988; 1995; Stankowska and Stankowski, 1988; Rotnicki and Borówka, 1995). The three main deglaciation phases defined based on morphostratigraphy were assigned to particular time intervals, e.g. ~20 ka BP, ~18.8 ka BP and ~16.2 ka BP for the Brandenburg, Frankfurt and Pomeranian Phases respectively (Kozarski, 1995). With the development of the radiocarbon

calibration curves (e.g., Reimer et al., 2004) it was possible to calibrate radiocarbon ages to calendar years, which constrained the age of the Brandenburg Phase to ~24 cal ka BP (Marks, 2012). Subsequent dating of glacial deposits with new methods such as OSL and/or cosmogenic nuclides (e.g., Wysota, et al., 2009; Marks, 2012; Tylmann et al., 2019) revealed that timing of the last SIS maximum extent is not synchronous, and in the area south of the Baltic Sea it may be correlated with the Brandenburg Phase in the western segment and the Frankfurt Phase in the eastern segment of the ice margin.

Here we presented geochronological evidences that the age of the Pomeranian ice-marginal belt, which was traditionally correlated with a discrete time interval during the last deglaciation (the “Pomeranian Phase”), covers in fact a relatively wide time window between 20 ka and 15 ka. We suggest that the “Pomeranian Phase”, which terminology originated based on morphostratigraphy and relative chronology observations, is in fact not a discrete time interval during the last deglaciation (a phase in terms of chronostratigraphy), but rather, a purely morphostratigraphic unit. Thus, we argue that the term “Pomeranian Phase” should not be used and that the terms “Pomeranian moraines” or “Pomeranian ice-marginal belt” are more adequate to describe the geomorphological record of the palaeo-ice margin positions which occurred during various phases of the last deglaciation. This also implies the potential need to revise the entire pattern of deglaciation stages/phases in the southern periphery of the SIS after its last maximum extent. This revision should be approached by confronting the available geochronological data with the existing framework of palaeo-ice margin positions (Fig. 6B). The revision may be based on a new geomorphological analysis of ice-marginal zones inferred from high-resolution digital elevation models linked with a Bayesian approach to integrate geochronological data and model ages for particular ice margin positions to capture the dynamics of particular ice margin oscillations and reconstruct a comprehensive retreat pattern for the southern periphery of the last SIS.

6. Conclusions

Our study provides the largest dataset for a direct chronology of the southern periphery of the last SIS associated with the Pomeranian ice-marginal belt. A new set of 25 ¹⁰Be surface exposure ages of boulders located on the Pomeranian moraines and of erratic boulders located directly upstream of the Pomeranian moraines in northern Poland. Together with recalculated ¹⁰Be surface exposure ages along the Pomeranian ice-marginal belt in the European Lowland we document a clear asynchrony of the ice margin positions with about 3–5 ka difference between the Bælthav ice margin in Denmark and the Braslav ice margin in Belarus. Our best age estimates constrain deposition of the Pomeranian ice-marginal formations to discrete intervals: (1) ~20–19 ka in the area of the Baltic Ice Stream, (2) ~19–18 ka in the area of the Odra Ice Stream, (3) ~20–19 ka in the interstream zone between the Odra and the Vistula Ice Streams, (4) ~19–18 ka in the area of the Vistula Ice Stream, (5) ~18–17 ka in the area of the Mazury Ice Stream, (6) ~17–16 ka in the area of the Riga Ice Stream, and (7) ~16–15 ka in the area of the Novgorod Ice Stream. The time-transgressive character of the Pomeranian ice-marginal belt was most likely caused by spatial and temporal variability of the last SIS dynamics triggered by activation and deactivation of particular ice streams.

The time-slice reconstruction of the last SIS's southern fringe inferred from the age constraints of the ice margin positions reveals a new scenario of the ice sheet evolution over the ~20–15 ka period. The southern periphery of the last SIS during this period is characterized by a clear temporal asymmetry: the western sector retreated earlier and much further to the north from the

Pomeranian ice-marginal belt than the eastern sector. The more dynamic behavior of the western sector compare to the eastern sector of the ice margin might result from the maritime climate in the west, the abundance of tidewater ice margins, and/or the dominance of warm-based ice in the western sector of the southern SIS.

The age of the Pomeranian ice-marginal belt, which formation was traditionally correlated with a discrete time interval of the last deglaciation (the “Pomeranian Phase”), covers actually a relatively wide time window (20–15 ka). This means that the “Pomeranian Phase”, which originated from morphostratigraphy and relative chronology of deglaciation, in fact is not a discrete time interval during the last deglaciation, but rather purely morphostratigraphic unit. Thus, the term “Pomeranian Phase” should not be used and the terms “Pomeranian moraines” or “Pomeranian ice-marginal belt” are adequate to describe geomorphological record of the palaeo-ice margin positions which occurred during various phases of the last deglaciation.

Funding

This work was supported by the National Science Center in Poland [grant no. 2014/15/D/ST10/04113 to Karol Tylmann]. The ASTER AMS national facility (CEREGE, Aix-en-Provence) is supported by the INSU/CNRS, the ANR through the “Projets thematiques d'excellence” program for the “Equipements d'excellence” ASTER-CEREGE action and IRD.

Samples MVP, BER, POM, PM, POL, BALTI, LIT and BEL measured at the ASTER facility (Rinterknecht et al., 2006; this study). Samples SJAE, FYN and JYL measured at the SUERC AMS Laboratory (Houmark-Nielsen et al., 2012). Samples PO measured at the PSI/ETH Zürich tandem accelerator facility (Heine et al., 2009). AMS $^{10}\text{Be}/^9\text{Be}$ results are standardized to NIST SRM 4325 (samples POM, POL, BALTI, LIT, BEL, SJAE, FYN and JYL), STD-11 (samples MVP, BER, PM) and S555 (samples PO) standards. $^{10}\text{Be}/^9\text{Be}$ ratios were corrected for a process blank values of 3.8×10^{-15} (samples POM, POL, BALTI, LIT, BEL), 1.3×10^{-15} (samples MVP), from 2.9 to 13.2×10^{-15} (samples SJAE, FYN and JYL) and 4.44×10^{-15} (samples PM). Exposure ages were calculated using a standard atmosphere and a rock density of 2.7 g/cm^3 .

Author contribution

The contribution of co-authors to the manuscript is the following: K. Tylmann – conceptualization, collecting data, data analysis, interpreting and discussing results, writing (first draft, editing and proof-reading), V.R. Rinterknecht - collecting data, data analysis, writing (editing and proof-reading), P.P. Woźniak - collecting data, writing (editing and proof-reading), V. Guillou and ASTER Team (Georges Aumaître, Didier L. Bourlès and Karim Keddadouche) – samples analysis.

Declaration of competing interest

The authors declare that they have no known competing financial interests or personal relationships that could have influenced the work reported in this paper.

Data availability

Data will be made available on request.

Acknowledgements

We are very grateful to the Regional Directorates of

Environmental Protection local communes offices for permissions for sampling large erratics protected by law. We appreciate constructive suggestions of an anonymous reviewer and of Eiliv Larsen which helped to improve the manuscript.

References

- Alley, R.B., 2004. GISP2 Ice Core Temperature and Accumulation Data. IGBP PAGES/World Data Center for Paleoclimatology Data Contribution Series #2004-013. NOAA/NGDC Paleoclimatology Program, Boulder CO, USA.
- Andrén, T., 2012. Baltic sea basin, since the latest deglaciation. In: Bengtsson, L., Herschy, R.W., Fairbridge, R.W. (Eds.), *Encyclopedia of Lakes and Reservoirs. Encyclopedia of Earth Sciences Series*. Springer, Dordrecht.
- Arnold, M., Merchel, S., Bourlès, D.L., Braucher, R., Benedetti, L., Finkel, R.C., Aumaître, G., Gottdang, A., Klein, M., 2010. The French accelerator mass spectrometry facility ASTER: improved performance and developments. *Nucl. Instrum. Methods Phys. Res. B* 268, 1954–1959.
- Balco, G., Stone, J.O., Lifton, N.A., Dunai, T.J., 2008. A complete and easily accessible means of calculating surface exposure ages or erosion rates from ^{10}Be and ^{26}Al measurements. *Quat. Geochronol.* 3, 174–195.
- Barth, A.M., Marcott, S.A., Licciardi, J.M., Shakun, J.D., 2019. Deglacial thinning of the Laurentide ice sheet in the Adirondack Mountains, New York, USA, revealed by ^{36}Cl exposure dating. *Paleoceanogr. Paleoclimatol.* 34, 946–953.
- Blomdin, R., Stroeven, A.P., Harbor, J.M., Lifton, N.A., Heyman, J., Gribenski, N., Caffee, M.W., Ivanov, M.N., Hättestrand, C., Rogozhina, I., Usabaliev, R., 2016. Evaluating the timing of former glacier expansions in the Tian Shan: a key step towards robust spatial correlations. *Quat. Sci. Rev.* 153, 78–96.
- Błaszkiwicz, M., 1998. The Wierzyca Valley, its Genesis and Development in Late Pleistocene and Early Holocene (In Polish with English Summary), vol. 10. Dokument. Geogr.
- Błaszkiwicz, M., 2011. Timing of the final disappearance of permafrost in the central European Lowland, as reconstructed from the evolution of lakes in N Poland. *Geol. Q.* 55, 361–374.
- Borchers, B., Marrero, S., Balco, G., Caffee, M., Goehring, B., Lifton, N., Nishiizumi, K., Philips, F., Schaefer, J., Stone, J., 2016. Geological calibration of spallation production rates in the CRONUS-Earth project. *Quat. Geochronol.* 31, 188–198.
- Boulton, G.S., Dongelmans, P., Punkari, M., Broadgate, M., 2001. Pleistogeology of an ice sheet through a glacial cycle: the European ice sheet through the Weichselian. *Quat. Sci. Rev.* 20, 591–625.
- Böse, M., 2005. The last glaciation and geomorphology. In: Koster, E.A. (Ed.), *The Physical Geography of Western Europe*. Oxford University Press, pp. 61–74.
- Braucher, R., Guillou, V., Bourlès, D.L., Arnold, M., Aumaître, G., Keddadouche, K., Nottoli, E., 2015. Preparation of ASTER in-house $^{10}\text{Be}/^9\text{Be}$ standard solutions. *Nucl. Instrum. Methods Phys. Res. B* 361, 335–340.
- Bremer, F., 2000. Geologische Übersichtskarte von Mecklenburg-Vorpommern 1: 500.000. LUNG M-V, Güstrow.
- Cepek, A., 1965. Geologische Ergebnisse der ersten Radiokarbonatierungen von Interstadialen im Lausitzer Urstromtal. *Geologie* 14, 625–657.
- Chmeleff, J., von Blanckenburg, F., Kossert, K., Jakob, D., 2010. Determination of the ^{10}Be half-life by multicollector ICP-MS and liquid scintillation counting. *Nucl. Instrum. Methods Phys. Res. Sect. B Beam Interact. Mater. Atoms* 268, 192–199.
- Clark, J., McCabe, C.M., Schnabel, C., Clark, P.U., Freedman, S.P.H.T., Maden, C., Xu, S., 2009. Cosmogenic ^{10}Be chronology of the last deglaciation of western Ireland, and implications for sensitivity of the Irish Ice Sheet to climate change. *Geol. Soc. Am. Bull.* 121, 3–16.
- Corbett, L.B., Bierman, P.R., Larsen, P., Stone, B.D., Caffee, M.W., 2017. Cosmogenic nuclide age estimate for Laurentide Ice Sheet recession from the terminal moraine, New Jersey, USA, and constraints on Latest Pleistocene ice sheet behavior. *Quat. Res.* 87, 482–498.
- Czernik, J., 2009. Radiocarbon dating of Late Glacial sediments of Lake Miłkowskie by accelerator mass spectrometry. *Acta Palaeobot.* 49, 337–352.
- Dulfer, H., Margold, M., Engel, Z., Braucher, R., 2021. Using ^{10}Be dating to determine when the Cordilleran ice sheet stopped flowing over the Canadian Rocky Mountains. *Quat. Res.* 102, 222–233. ASTER Team.
- Ehlers, J., Grube, A., Stephan, H.-J., Wansa, S., 2011. Pleistocene glaciations of north Germany—new results. In: Ehlers, J., Gibbard, P.L., Hughes, P.D. (Eds.), *Quaternary Glaciations - Extent and Chronology: A Closer Look*. Elsevier Amsterdam, pp. 149–162.
- Galon, R., Roszkówna, L., 1961. Extents of the Scandinavian glaciations and of their recession stages on the Territory of Poland in the light of an analysis of the marginal forms of inland ice. *Przeglad Geogr.* 33, 347–361.
- Gatka, M., Sznaj, M., 2013. Late Glacial and Early Holocene development of lakes in northeastern Poland in view of plant macrofossil analyses. *Quat. Int.* 292, 124–135.
- Gorlach, A., Hang, T., Kalm, V., 2017. GIS-based reconstruction of Late Weichselian proglacial lakes in northwestern Russia and Belarus. *Boreas* 46, 486–502.
- Guobytė, R., 2004. A brief outline of the Quaternary of Lithuania and the history of its investigation. In: Ehlers, J., Gibbard, P.L. (Eds.), *Quaternary Glaciations - Extent and Chronology, Part I: Europe*. Elsevier, Amsterdam, pp. 245–250.
- Guobytė, R., Satkūnas, J., 2011. Pleistocene glaciations in Lithuania. In: Ehlers, J., Gibbard, P.L., Hughes, P.D. (Eds.), *Quaternary Glaciations - Extent and Chronology: A Closer Look. Developments in Quaternary Science*, vol. 15. Elsevier, Amsterdam, pp. 231–246.

- Heine, K., Reuther, A.U., Thieke, H.U., Schulz, R., Schlaak, N., Kubik, P.W., 2009. Timing of Weichselian ice marginal positions in Brandenburg (northeastern Germany) using cosmogenic in situ ¹⁰Be. *Z. Geomorphol. NF* 53, 433–454.
- Hermanowski, P., 2015. Substratum morphology and significance during the Weichselian Odra ice lobe advance in northeast Germany and northwest Poland. *Geologos* 21, 241–248.
- Houmark-Nielsen, M., 2007. Extent and age of Middle and Late Pleistocene glaciations and periglacial episodes in southern Jylland, Denmark. *Bull. Geol. Soc. Den.* 55, 9–35.
- Houmark-Nielsen, M., 2011. Pleistocene glaciations in Denmark: a closer look at chronology, ice dynamics and landforms. In: Ehlers, J., Gibbard, P.L., Hughes, P.D. (Eds.), *Quaternary Glaciations – Extent and Chronology: A Closer Look. Developments in Quaternary Science*, vol. 15. Elsevier, Amsterdam, pp. 47–58.
- Houmark-Nielsen, M., Kjær, K.H., 2003. Southwest Scandinavia, 40–15 kyr BP: palaeogeography and environmental change. *J. Quat. Sci.* 18, 769–786.
- Houmark-Nielsen, M., Linge, H., Fabel, D., Schnabel, C., Xu, S., Wilcken, K.M., Binnie, S., 2012. Cosmogenic surface exposure dating the last deglaciation in Denmark: discrepancies with independent age constraints suggest delayed periglacial landform stabilisation. *Quat. Geochronol.* 13, 1–13. <https://doi.org/10.1016/j.quageo.2012.08.006>.
- Hughes, A.L.C., Gyllencreutz, R., Lohne, Ø.S., Mangerud, J., Svendsen, I.J., 2016. The last Eurasian ice sheets - a chronological database and time-slice reconstruction, DATED-1. *Boreas* 45, 1–45.
- Hughes, A.L.C., Winsborrow, M.C.M., Greenwood, S.L., 2021. European ice sheet complex evolution during the last glacial maximum (29–19 ka). In: Palacios, D., Hughes, P.D., García-Ruiz, J.M., Andrés, N. (Eds.), *European Glacial Landscapes. Maximum Extent of Glaciations*. Elsevier, pp. 361–372.
- Ivy-Ochs, S., Kober, F., 2008. Surface exposure dating with cosmogenic nuclides. *Eiszeitl. Ggw. Q. Sci. J.* 57, 179–209.
- Kalm, V., 2006. Pleistocene chronostratigraphy in Estonia, southeastern sector of the Scandinavian glaciation. *Quat. Sci. Rev.* 25, 960–975.
- Karabanov, A.K., Matveyev, A.V., 2011. The Pleistocene glaciations in Belarus. In: Ehlers, J., Gibbard, P.L., Hughes, P.D. (Eds.), *Quaternary Glaciations – Extent and Chronology: A Closer Look. Developments in Quaternary Science*, vol. 15. Elsevier, Amsterdam, pp. 29–35.
- Karabanov, A.K., Matveyev, A.V., Pavlovskaya, I.E., 2004. The main glacial limits in Belarus. In: Ehlers, J., Gibbard, P.L. (Eds.), *Quaternary Glaciations: Extent and Chronology*. Elsevier B.V., Amsterdam, pp. 15–18.
- Karczewski, A., 1989. Morphogenesis of the Ice-Marginal Zone of the Pomeranian Phase in the Area of the Parsęta Ice Lobe during Vistulian (Middle Pomerania). University of Adam Mickiewicz Press, Poznań, Geography Series, p. 44 (in Polish).
- Keilhack, K., 1901. Geologisch-Morphologische Übersichtskarte der Provinz Pommern. 1:500 000. Königl. Preuss. Geol. Landesanst. u. Bergakad., Berlin.
- Keilhack, K., 1909. Begleitworte zur Karte der Endmoränen und Urstromtäler Norddeutschlands. *Jahrbuch Konigl. Preufs. Geol. Landesanst.* XXX 507–510.
- Kenzler, M., Tsukamoto, S., Meng, S., Thiel, C., Frechen, M., Hüneke, H., 2015. Luminescence dating of Weichselian interstadial sediments from the German Baltic Sea coast. *Quat. Geochronol.* 30, 215–256.
- Kenzler, M., Tsukamoto, S., Meng, S., Frechen, M., Hüneke, H., 2017. New age constraints from the SW Baltic Sea area – implications for Scandinavian Ice Sheet dynamics and palaeoenvironmental conditions during MIS 3 and early MIS 2. *Boreas* 46, 34–52.
- Klysz, P., 2003. Maximum limits of the Baltic ice-sheet during the Pomeranian phase in the Drawskie Lakeland. *Quaest. Geogr.* 22, 29–42.
- Kordowski, J., 2009. On the Lower Vistula Valley development in the light of geomorphological and sedimentological investigations. *Pol. Geol. Inst. Spec. Pap.* 25, 21–36.
- Korschinek, G., Bergmaier, A., Faestermann, T., Gerstmann, U.C., Knie, K., Rugel, G., Wallner, A., Dillmann, I., Dollinger, G., von Gostomski, C.L., 2010. A new value for the half-life of ¹⁰Be by Heavy-Ion Elastic Recoil Detection and liquid scintillation counting. *Nucl. Instrum. Methods Phys. Res. Sect. B Beam Interact. Mater. Atoms* 268, 187–191.
- Kozarski, S., 1981. Vistulian stratigraphy and chronology of the Great Poland Lowland. *Geografia* 6, 1–44.
- Kozarski, S., 1988. Time and dynamics of the last Scandinavian ice-sheet retreat from northwestern Poland. *Geogr. Pol.* 55, 91–101.
- Kozarski, S., 1995. Deglaciation of northwestern Poland: environmental conditions and geosystem transformation (~20 ka – 10 ka BP). *Dok. Geogr.* 1, 1–82 (in Polish with English summary).
- Krohn, C.F., Larsen, N.K., Kronborg, C., Nielsen, O.B., Knudsen, K.L., 2009. Litho- and chronostratigraphy of the Late Weichselian in Vendsyssel, northern Denmark with special emphasis on tunnel-valley infill in relation to a receding ice margin. *Boreas* 38, 811–833.
- Lagerlund, E., Houmark-Nielsen, M., 1993. Timing and pattern of the last deglaciation in the Kattegat region, southwest Scandinavia. *Boreas* 22, 337–347.
- Lauterbach, S., Brauer, A., Andersen, N., Danielopol, D.L., Dulski, P., Hüls, M., Milecka, K., Namiotko, T., Plessen, B., Von Grafenstein, U., Participants, DecLakes, 2011. Multi-proxy evidence for early to mid-Holocene environmental and climatic changes in northeastern Poland. *Boreas* 40, 57–72.
- Lal, D., 1991. Cosmic ray labeling of erosion surfaces: in situ nuclide production rates and erosion models. *Earth Planet. Sci. Lett.* 104, 424–439.
- Larsen, E., Fredin, O., Jensen, M., Kuznetsov, D., Lyså, A., Subetto, D., 2014. Subglacial sediment, proglacial lake-level and topographic controls on ice extent and lobe geometries during the Last Glacial Maximum in NW Russia. *Quat. Sci. Rev.* 92, 369–387.
- Larsen, E., Fredin, O., Lyså, A., Amantov, A., Fjeldskaar, W., Ottesen, D., 2016. Causes of time-transgressive glacial maxima positions of the last Scandinavian Ice Sheet. *Norw. J. Geol.* 96, 159–170.
- Larsen, N.K., Knudsen, K.L., Krohn, C.F., Ronborg, C., Murray, A.S., Nielsen, O.B., 2009. Late Quaternary ice sheet, lake and sea history of southwest Scandinavia – a synthesis. *Boreas* 38, 732–761.
- Lasberg, K., Kalm, V., 2013. Chronology of late Weichselian glaciation in the western part of the east European plain. *Boreas* 42, 995–1007.
- Liedtke, H., 1975. Die nordischen vereisungen in Mitteleuropa. *Forsch. Dtsch. Landeskd.* 204 (Bonn–Bad Godesberg).
- Liedtke, H., 2001. Das nordöstliche Brandenburg während der Weichseleiszeit. In: Bussemer, S. (Ed.), *Das Erbe der Eiszeit*. Beier & Beran, Langenweissbach, pp. 119–133.
- Litt, T., Behre, K.E., Meyer, K.D., Stephan, H.J., Wansa, S., 2007. Stratigraphische Begriffe für das Quartär des norddeutschen Vereisungsgebietes. *E G Q. Sci. J.* 56, 7–65.
- Lundqvist, J., Wohlfarth, B., 2001. Timing and east-west correlation of south Swedish ice marginal lines during the Late Weichselian. *Quat. Sci. Rev.* 20, 1127–1148.
- Lüthgens, C., Böse, M., 2012. From morphostratigraphy to geochronology – on the dating of ice marginal positions. *Quat. Sci. Rev.* 44, 26–36.
- Lüthgens, C., Böse, M., Preusser, F., 2011. Age of the Pomeranian ice-marginal position in northeastern Germany determined by Optically Stimulated Luminescence (OSL) dating of glaciofluvial sediments. *Boreas* 40, 598–615.
- Marks, L., 2002. Last glacial maximum in Poland. *Quat. Sci. Rev.* 21, 103–110.
- Marks, L., 2012. Timing of the late vistulian (Weichselian) glacial phases in Poland. *Quat. Sci. Rev.* 44, 81–88.
- Marks, L., 2015. Last deglaciation of northern Continental Europe. *Cuadernos Investig. Geogr.* 41, 279–297.
- Marsella, K.A., Bierman, P.R., Davis, P.T., Caffee, M.W., 2000. Cosmogenic Be-10 and Al-26 ages for the last glacial maximum, eastern Baffin Island, Arctic Canada. *Geol. Soc. Am. Bull.* 112, 1296–1312.
- Merchel, S., Arnold, M., Aumaitre, G., Benedetti, L., Bourlès, D.L., Braucher, R., Alfimov, V., Freeman, S.P.H.T., Steier, P., Wallner, A., 2008. Towards more precise ¹⁰Be and ³⁶Cl data from measurements at the 10–14 level: influence of sample preparation. *Nucl. Instrum. Methods Phys. Res. Sect. B Beam Interact. Mater. Atoms* 266, 4921–4926.
- Merchel, S., Herpers, U., 1999. An update on radiochemical separation techniques for the determination of long-lived radionuclides via accelerator mass spectrometry. *Radiochim. Acta* 84, 215–220.
- Mleczak, M., Pisarska-Jamroz, G., 2021. A record of deglaciation-related shifting of the proximal zone of a sandur – a case study from the Gwda sandur, NW Poland (MIS 2). *J. Palaeogeogr.* 10. <https://doi.org/10.1186/s42501-021-00089-x>.
- Mojski, J.E., 1986. Outline of the stratigraphy of north polish glaciation in north and Middle Poland. *Prace Geogr. Inst. Geogr. Pol. Akad. Nauk* 74, 37–64.
- Müller, U., Rühberg, N., Krienke, H.-D., 1995. The Pleistocene sequence in Mecklenburg-vorpommern. In: Ehlers, J., Kozarski, S., Gibbard, P.L. (Eds.), *Glacial Deposits in North-East Europe*. Balkema A.A. Publishers, Rotterdam, pp. 501–514.
- Neustadt, M., 1971. About the lower boundary of the Holocene. In: Neustadt, M. (Ed.), *Palynology of the Holocene*. Institut Geografii Akademii Nauk SSSR (Academy of Sciences of the USSR Publishers), Moscow, pp. 7–13.
- Niewiarowski, W., 2003. Pleniglacial and Late Vistulian glacial lakes, their sediments and landforms: a case study from the young glacial landscape of Northern Poland. *Prace Geogr.* 128, 133–142.
- Pachucki, C., 1961. Moreny Czołowe Ostatniego Zlodowacenia Na Obszarze Peribalticum, vol. XXXI. *Rocznik Polskiego Towarzystwa Geologicznego Annales De La Societe Geologique De Pologne*, pp. 303–318.
- Patton, H., Hubbard, A., Andreassen, K., Auriac, A., Whitehouse, P.L., Stroeven, A.P., Shackleton, C., Winsborrow, M., Heyman, J., Hall, A.M., 2017. Deglaciation of the Eurasian ice sheet complex. *Quat. Sci. Rev.* 169, 148–172.
- Philippson, B., 2013. The freshwater reservoir effect in radiocarbon dating. *Heritage Sci.* 1, 1–24.
- Pisarska-Jamroz, M., Belzyt, S., Börner, A., Hoffmann, G., Hüneke, H., Kenzler, M., Obst, K., Rother, H., van Loon, A.J., 2018. Evidence from seismites for glacio-isostatically induced crustal faulting in front of an advancing land-ice mass (Rügen Island, SW Baltic Sea). *Tectonophysics* 745, 338–348.
- Punkari, M., 1995. Function of the ice streams in the Scandinavian ice sheet: analyses of glacial geological data from southwestern Finland. *Trans. R. Soc. Edinb. Earth Sci.* 85, 283–302.
- Punkari, M., 1997. Glacial and glaciofluvial deposits in the interlobate areas of the Scandinavian ice sheet. *Quat. Sci. Rev.* 16, 741–753.
- Raukas, A., Stankowski, W., Zelcs, V., Sinkunas, P., 2010. Chronology of the last deglaciation in the southeastern Baltic region on the basis of recent OSL dates. *Geochronometria* 36, 47–54.
- Reimer, P.J., Austin, W.E.N., Bard, E., Bayliss, A., Blackwell, P.G., Bronk Ramsey, C., Butzin, M., Cheng, H., Edwards, R.L., Friedrich, M., Grootes, P.M., Guilderson, T.P., Hajdas, I., Heaton, T.J., Hogg, A.G., Hughen, K.A., Kromer, B., Manning, S.W., Muscheler, R., Palmer, J.G., Pearson, C., van der Plicht, J., Reimer, R.W., Richards, D.A., Scott, E.M., Southon, J.R., Turney, C.S.M., Wacker, L., Adolphi, F., Büntgen, U., Capano, M., Fahrni, S.M., Fogtmann-Schulz, A., Friedrich, R., Köhler, P., Kudsk, S., Miyake, F., Olsen, J., Reinig, F., Sakamoto, M., Sookdeo, A., Talam, S., 2020. The IntCal20 northern hemisphere radiocarbon age calibration curve (0–55 cal ka BP). *Radiocarbon* 62, 725–757.

- Reimer, P.J., Baillie, M.G.L., Bard, E., Bayliss, A., Beck, J.W., Bertrand, C.J.K., Blackwell, P.G., Buck, C.E., Burr, G.S., Cutler, K.B., Damon, P.E., Edwards, R.L., Fairbanks, R.G., Friedrich, M., Guilderson, T.P., Hogg, A.G., Hughen, K.A., Kromer, B., McCormac, G., Manning, S., Ramsey, C.B., Reimer, R.W., Remmelle, S., Southon, J.R., Stuiver, M., Talamo, S., Taylor, F.W., Van der Plicht, J., Weyhenmeyer, C.E., 2004. IntCal04 terrestrial radiocarbon age calibration, 0–26 cal kyr BP. *Radiocarbon* 46, 1029–1058.
- Rinterknecht, V.R., Börner, A., Bourlès, D., Braucher, R., 2014. Cosmogenic ^{10}Be dating of ice sheet marginal belts in Mecklenburg-Vorpommern, Western Pomerania (northeast Germany). *Quat. Geochronol.* 19, 42–51.
- Rinterknecht, V., Braucher, R., Böse, M., Bourlès, D., Mercier, J.L., 2012. Late Quaternary ice sheet extents in northeastern Germany inferred from surface exposure dating. *Quat. Sci. Rev.* 44, 89–95.
- Rinterknecht, V.R., Clark, P.U.M., Raisbeck, G.M., Yiou, F., Bitinas, A., Brook, E.J., Marks, L., Zelcs, V., Lunkka, J.P., Pavlovskaya, I.E., Piotrowski, J.A., Rauskas, A., 2006. The last deglaciation of the southeastern sector of the Scandinavian Ice Sheet. *Science* 311, 1449–1452.
- Rinterknecht, V., Hang, T., Gorchach, A., Kohv, M., Kalla, K., Kalm, V., Subetto, D., Bourlès, D., Léanni, L., Guillou, V., 2018. The last glacial maximum extent of the Scandinavian ice sheet in the Valday heights, western Russia: evidence from cosmogenic surface exposure dating using ^{10}Be . *Quat. Sci. Rev.* 200, 106–113. ASTER Team.
- Roman, M., 1990. Zlodowacenie Wisły w rejonie Bramki w zachodniej części Pojezierza Mazurskiego. *Kwart. Geol.* 34, 325–338.
- Rosko, L., 1955. End moraines of the western Mazurian lake country. *Stud. Soc. Sci. Turunen.* 2, 35–245.
- Roszkówna, L., 1968. Recesja ostatniego lądolodu z terenu Polski. In: Galon, R. (Ed.), *Ostatnie Zlodowacenie Skandynawskie W Polsce*, vol. 74. Pr. Geogr. Inst. Geogr. PAN, pp. 65–100.
- Rotnicki, K., Borówka, R.K., 1995. The last cold period in the Gardno-Leba coastal plain. *J. Coast Res.* 22, 225–229.
- Serebryanny, L.R., 1978. *The Dynamics of Continental Ice Sheet and Glacio-Eustasy in the Late Quaternary Time*. Nauka, Moscow.
- Small, D., Benetti, S., Dove, D., Ballantyne, C.K., Fabel, D., Clark, C.D., Gheorghiu, D.M., Newall, J., Xu, S., 2017. Cosmogenic exposure age constraints on deglaciation and flow behavior of a marine-based ice stream in western Scotland, 21–16 ka. *Quat. Sci. Rev.* 167, 30–46.
- Stankowska, A., Stankowski, W., 1988. Maximum extent of the Vistulian ice sheet in the vicinity of Konin, Poland: a geomorphologic, sedimentological and radiometric evidence. *Geogr. Pol.* 55, 141–150.
- Stokes, C.R., Clark, C.D., 1999. Geomorphological criteria for identifying Pleistocene ice streams. *Ann. Glaciol.* 28, 67–74.
- Stone, J., 2000. Air pressure and cosmogenic isotope production. *J. Geophys. Res.* 105, 23753–23760.
- Stroeven, A.P., Hättestrand, C., Kleman, J., Heyman, J., Fabel, D., Fredin, O., Goodfellow, B.W., Harbor, J.M., Jansen, J.D., Olsen, L., Caffee, M.W., Fink, D., Lundqvist, J., Rosqvist, G.C., Strömberg, B., Jansson, K.N., 2016. Deglaciation of fennoscandia. *Quat. Sci. Rev.* 147, 91–121.
- Tylmann, K., Rinterknecht, V.R., Woźniak, P.P., Bourlès, D., Schimmelpfennig, I., Guillou, V., 2019. The local last glacial maximum of the southern Scandinavian ice sheet front: cosmogenic nuclide dating of erratics in northern Poland. *Quat. Sci. Rev.* 219, 36–46. ASTER Team.
- Tylmann, K., Uścińowicz, Sz., 2022. Timing of the last deglaciation phases in the southern Baltic area inferred from Bayesian age modeling. *Quat. Sci. Rev.* 287, 107563.
- Uścińowicz, Sz., 1999. Southern Baltic area during the last deglaciation. *Geol. Q.* 43, 137–148.
- Uścińowicz, Sz., Adamiec, G., Bluszcz, A., Jegliński, W., Jurys, L., Miotk-Szpiganowicz, G., Moska, P., Pączek, U., Piotrowska, P., Poręba, G., Przedziecki, P., Uścińowicz, G., 2019. Chronology of the last ice sheet decay on the southern Baltic area based on dating of glaciofluvial and ice-dammed lake deposits. *Geol. Q.* 63, 192–207.
- Wanschaffe, F., 1908. *Die Umstromtaller Norddeutschlands die Endmoränen und Fundorte der Glacialschrammen*. In: Meyers Großes Konversations-Lexikon, vol. 14. Leipzig.
- Woldstedt, P., 1925. Die großen endmoränenzüge norddeutschlands. *Z. Dtsch. Geol. Ges.* 77, 172–184.
- Woldstedt, P., 1935. *Geologisch-morphologische Übersichtskarte des norddeutschen Vereisungsgebietes*. Preußische Geologische Landesanstalt, Berlin.
- Wysota, W., 1999. Ice sheet maximum limit of the vistulian glaciation in the mid-eastern Chelmino–Dobrzyń Lakeland, northern Poland. *Geol. Q.* 43, 189–202.
- Wysota, W., Molewski, P., Sokołowski, R.J., 2009. Record of Vistula ice lobe advance in the Late Weichselian glacial sequence in north-central Poland. *Quat. Int.* 207, 26–41.
- Zimenkov, O., 1989. Age of the maximum extent of the Poozerian Glaciation in Belarus. New data about Cenozoic geology of Belarus and adjacent areas. In: Matveyev, A. (Ed.), *Nauka i Tekhnika*, Minsk, Belarus, pp. 30–44 (in Russian).